OAK RIDGE NATIONAL LABORATORY LIBRARY
3 4456 0021460 3

ORNL/TM-5789

Cy. 1

Dislocation Loop Growth and Void Swelling in Bounded Media by Charged Particle Damage

M. H. Yoo

OAK RIDGE NATIONAL LABORATORY
CENTRAL RESEARCH LIBRARY
DOCUMENT COLLECTION
LIBRARY LOAN COPY
DO NOT TRANSFER TO ANOTHER PERSON
If you find someone else is using this
document, send it along with document
and the library will arrange a loan.

OAK RIDGE NATIONAL LABORATORY
OPERATED BY UNION CARBIDE CORPORATION FOR THE ENERGY RESEARCH AND DEVELOPMENT ADMINISTRATION

Printed in the United States of America
National Technical Information Service
U.S. Department of Commerce
5285 Port Royal Road, Springfield, Virginia 22161
Price: Printed Copy $[illegible]; Microfiche $[illegible]

This report was prepared as an account of work sponsored by the United States Government. Neither the United States nor the United States Nuclear Regulatory Commission, nor any of their employees, nor any of their contractors, subcontractors, or their employees, makes any warranty, express or implied, or assumes any legal liability or responsibility for the accuracy, completeness or usefulness of any information, apparatus, product or process disclosed, or represents that its use would not infringe privately owned rights.

ORNL/TM-5789
Distribution
Category UC-25

Contract No. W-7405-eng-26

METALS AND CERAMICS DIVISION

DISLOCATION LOOP GROWTH AND VOID SWELLING IN BOUNDED MEDIA BY CHARGED PARTICLE DAMAGE

M. H. Yoo

Date Published - April 1977

OAK RIDGE NATIONAL LABORATORY
Oak Ridge, Tennessee 37830
operated by
UNION CARBIDE CORPORATION
for the
ENERGY RESEARCH AND DEVELOPMENT ADMINISTRATION

OAK RIDGE NATIONAL LABORATORY LIBRARY
3 4456 0021460 3

CONTENTS

ABSTRACT 1
1. INTRODUCTION 1
2. THE RATE EQUATIONS 2
2.1 Growth Rate of Defect Clusters 2
2.1.1 Thermal Emission of Vancancies 3
2.1.2 Effective Capture Radius 5
2.1.2.1 Voids 6
2.1.2.2 Dislocations 7
2.1.2.3 Dislocation Loops 7
2.2 Point Defect Concentrations 8
2.2.1 Boundary Effects 8
2.2.2 Recombination Rate 9
2.2.3 Sink Strengths 9
2.2.4 Defect Generation Rate 11
3. SOLUTION OF THE RATE EQUATIONS 13
3.1 Initial and Boundary Conditions 13
3.2 Numerical Solutions 14
4. EXAMPLE CALCULATIONS 15
4.1 Recombination Dominant Case 16
4.2 Sink Dominant Case 18
4.3 General Case 21
5. SUMMARY AND DISCUSSION 24
6. REFERENCES 26
APPENDIX A 31
APPENDIX B 37
APPENDIX C 49

DISLOCATION LOOP GROWTH AND VOID SWELLING IN BOUNDED MEDIA BY CHARGED PARTICLE DAMAGE

M. H. Yoo

ABSTRACT

A system of partial differential rate equations for the growth of dislocation loops and voids in one-dimensionally bounded media, namely the semi-infinite medium and the foil, under charged particle irradiation has been formulated in terms of the diffusion controlled kinetics of defect annealing and cluster growth. An efficient numerical method of integrating the rate equations is presented. Example calculations for 4 MeV Ni self-ion bombardment at 550°C are made, and both time and space dependences of loop growth and void swelling are discussed.

---

1. INTRODUCTION

The investigation of microstructural radiation damage of metals by high-energy charged particles such as electrons, protons, and heavy ions has received considerable attention in recent years.[1-3] In the experimental study of void formation much effort is put into simulating the damage produced by fast neutrons in fission or fusion reactor conditions with that by heavy ion bombardment in an accelerator. In theoretical modeling of correlation of neutron and ion radiation damage mechanisms, only some of the important factors inherent to the ion bombardment situation have been incorporated into the homogeneous rate theory of void swelling.[4-6] Bullough et al.[7] extended the rate theory of void growth to include a homogeneous distribution of vacancy loops which may characterize the irradiation induced cascade damage. Taking the depth gradient of displacement damage by ion bombardment into account, Garner and Guthrie[8] solved the steady state rate equations for semi-infinite media and discussed the characteristics of depth dependent void growth. Transient solutions of the rate equations were obtained by Savino[9] for

thin foils under homogeneous displacement damage as in a high-voltage electron microscope. Ghoniem and Kulcinski[10] studied the growth behavior of voids and dislocation loops in an infinite medium under pulsed homogeneous displacement damage.

The purpose of the present paper is to present a general model of loop growth and void swelling in one-dimensionally bounded media during irradiation. It is assumed that annealing and clustering kinetics of point defects is diffusion controlled. Thin foils and semi-infinite media are considered. Both time and space dependences of the point defect generation rate, the concentrations of free point defects, and the sizes of fixed internal sinks are included in the model. In Sec. 2, a system of partial differential rate equations is formulated and physical meanings of the input parameters given. The numerical method used to integrate the rate euqtions is given in Sec. 3. Example calculations for the case of nickel self-ion bombardment on a semi-infinite medium is given in Sec. 4. Discussion follows in Sec. 5, which includes other possible applications of the present model.

2. THE RATE EQUATIONS

2.1 Growth Rate of Defect Clusters

Consider three different types of defect clusters as internal sinks for point defects such that

$$\rho_j = \rho_j(x,t) = R_j(x,t)/b \ , \tag{1}$$

where R_j is the average radius of jth sink type in the plane perpendicular to x-axis, x the distance from a reference boundary, t the time, and b is the Burgers vector of dislocation loops. We assign j = 1 for interstitial loops, j = 2 for vacancy loops, and j = 3 for voids. If one postulates that self-interstitials and vacancies are the only important free defects, then the growth rates of dislocation loops treated as spherical sinks and voids can be obtained from the net fluxes of point defects as follows:

$$\frac{\partial \rho_1}{\partial t} = \frac{2}{\rho_1 b^3}\left[r_i^{(1)} D_i C_i - r_v^{(1)} D_v (C_v - \overline{C}_1)\right] , \tag{2}$$

$$\frac{\partial \rho_2}{\partial t} = \frac{2}{\rho_2 b^3}\left[r_v^{(2)} D_v (C_v - \overline{C}_2) - r_i^{(2)} D_i C_i\right] , \tag{3}$$

$$\frac{\partial \rho_3}{\partial t} = \frac{1}{\rho_3 b^3}\left[r_v^{(3)} D_v (C_v - \overline{C}_3) - r_i^{(3)} D_i C_i\right] , \tag{4}$$

where subscripts v and i denote vacancies and interstitials, D's the diffusion coefficients, C's the fractional point defect concentrations, $r^{(j)}$ the effective capture radius of sink type (j) for point defects, and $\overline{C}_j$ is the local equilibrium concentration of vacancies at a sink of jth type.

When dislocation loops are large enough to be treated as dislocation line sinks, denoted by j = 4, the loop growth rates may be given as

$$\frac{\partial \rho_1}{\partial t} = \frac{1}{b^2}\left[Z_i D_i C_i - Z_v D_v \left(C_v - \overline{C}_1\right)\right] , \tag{5}$$

$$\frac{\partial \rho_2}{\partial t} = \frac{1}{b^2}\left[Z_v D_v \left(C_v - \overline{C}_2\right) - Z_i D_i C_i\right] , \tag{6}$$

where Z_v and Z_i are the numerical factors which depend on the effective capture radii, $r_{v,i}^{(4)}$, and the outer cut-off radius of dislocations.

2.1.1 Thermal Emission of Vacancies

In order for a faulted dislocation loop to be in local equilibrium with vacancies, the release of elastic line energy of the loop and the reduction of stacking fault energy must be related to the local concentration of thermal vacancies by

$$\overline{C}_1 = C_v^e \exp\left\{-\frac{\Omega}{bk_BT}\left[\gamma + \frac{\mu b}{4\pi(1-\nu)}\frac{\ln(\rho_1+1)}{(\rho_1+1)}\right]\right\} , \tag{7}$$

$$\overline{C}_2 = C_v^e \exp\left\{+\frac{\Omega}{bk_BT}\left[\gamma + \frac{\mu b}{4\pi(1-\nu)}\frac{\ln(\rho_2+1)}{(\rho_2+1)}\right]\right\} , \tag{8}$$

where Ω is the atomic volume, k_B is the Boltzmann's constant, T the absolute temperature, γ the stacking fault energy, μ the shear modulus, and ν is the Poisson's ratio. The thermal equilibrium value of vacancies is

$$C_v^e = \exp(S_v^f/k_B)\exp(-E_v^f/k_BT) , \tag{9}$$

where S_v^f and E_v^f are the entropy and energy of vacancy formation, respectively. For an unfaulted dislocation loop the stacking fault energy vanishes in Eqs. (7) and (8), and for a straight dislocation the line tension force also vanishes to give $\overline{C}_4 = C_v^e$.

Similarly, the local concentration of vacancies near a void is

$$\overline{C}_3 = C_v^e \exp\left[\frac{\Omega}{k_BT}\left(\frac{2\Gamma}{R_3} - P_g\right)\right] , \tag{10}$$

where Γ is the void surface energy and P_g is the gas pressure in each void of radius R_3. According to van der Waal's equation of state for non-interacting rigid gas atoms,

$$P_g = n_g k_BT/(4\pi R_3^3/3 - n_gB) , \tag{11}$$

where n_g is the number of gas atoms in a cavity of radius R_3 and B is van der Waal's coefficient. The number of gas atoms giving rise to an equilibrium pressure is

$$n_g = 8\pi\Gamma R_3^3/3(R_3 k_B T + 2\Gamma B) \ . \tag{12}$$

Unspecified so far, the radial distance from a sink at which $\overline{C}_j$ applies is the inner cut-off radius. To ensure a local thermodynamic equilibrium for vacancies one must include in Eqs. (7) and (8) the interaction energy between a vacancy and the sink at that radius as was done for infinitesimal loops in our earlier work.[11*] Because of the relatively weak strength, this interaction energy terms is neglected in the present model. The contribution of such an interaction term is substantial in the case of interstitials, but thermal emission of interstitials is neglected because of a large value of formation energy. Since $\overline{C}_j = \overline{C}_j(\rho_j)$ and $\rho_j = \rho_j(x,t)$ for j = 1, 2, 3, the local concentration of thermal vacancies is a function of position and time, $\overline{C}_j = \overline{C}_j(x,t)$.

2.1.2 Effective Capture Radius

The effective capture radius of an internal sink is defined by[11-14]

$$r_{v,i}^{(j)} = r_c^{(j)}\left(1 + \delta_{v,i}^{(j)}\right) \ , \tag{13}$$

where r_c is the capture radius and $\delta_{v,i}$ is the preference factor ($\delta \geqslant 0$). The magnitude of the preference factor is indicative of how strongly the point defects interact with the particular sink. Since the magnitude of the volume dilatation of an interstitial is greater than that of the relaxation volume of a vacancy, the first-order size interaction gives rise to the condition that $\delta_i > \delta_v$ for any sink type with a self-strain field. This condition is the primary cause of void formation at temperatures where both vacancies and interstitials are mobile.

---

*The following typographic errors in Eq. (6.8) of ref. 11 should be noted: the second and the third signs should be exchanged to read ± and +, respectively, and the last argument should contain 2 instead of 32.

2.1.2.1 Voids. As discussed earlier for randomly distributed spherical sinks,[11,12] the capture radius of a typical void may be approximated by

$$r_c = \frac{r_1 r_2}{r_2 - r_1} , \tag{14}$$

where the superscript (j) is omitted for brevity, r_1 is the inner cut-off radius, the void radius in this case, and r_2 is the radius of the outer boundary which can be assumed to be, $r_2 = (r_1 + R_s)/2$, the average of r_1 and the radius of the sphere of influence, $R_s = (3/4\pi N)^{1/3}$, where N is the void number density.

Brailsford et al.[15] have recently derived a simplified expression for the sink strength of voids, which duplicates reasonably well the procedure given by Brailsford and Bullough.[6] Bringing the 'effective lossy medium' right up to the void, i.e., $R_s = r_1$, they[15] eliminate the problem of defining R_s when more than one sink type is present. According to their expression for the sink strength for voids as the only sink, the capture radius of voids is

$$r_c = r_1 F^2 , \tag{15a}$$

$$F = \left[1 + \left(\frac{1}{2}\lambda r_1\right)^2\right]^{1/2} + \frac{1}{2}\lambda r_1 , \tag{15b}$$

$$\lambda = (4\pi r_1 N)^{1/2} . \tag{15c}$$

The capture radius evaluated from Eqs. (15) is smaller than that from Eq. (14). As expected from the many sink effect, the difference between the two increases as the void size and the void number density increase. For the example calculations in the present work, Eqs. (15) are used to evaluate the capture radii of spherical sinks.

2.1.2.2 Dislocations. The term 'effective capture radius' was coined first by Ham[12] in his work on particle precipitation on dislocations. The capture radius in Eq. (13), $r_c^{(4)}$, is equivalent to the dislocation core radius, r_d, and the preference factor, $\delta_{v,i}^{(4)}$, denotes the effect of point defect-dislocation interaction on defect flux. For a random distribution of straight parallel dislocations, the numerical factors given in Eqs. (5) and (6) may be related to the effective capture radius by[16]

$$Z_v = 2\pi/\ln(R_c/r_v^{(4)}) \quad , \tag{16a}$$

$$Z_i = 2\pi/\ln(R_c/r_i^{(4)}) \quad , \tag{16b}$$

where $R_c = (\pi L)^{-1/2}$, L is the dislocation line density. A similar correction as for Eqs. (15) to Eq. (14) was also made to Eqs. (16) by Brailsford et al.[15] but this is not included in the present work.

2.1.2.3 Dislocation Loops. When dislocation loops are randomly distributed and are small compared to their sphere of influence, the torus of a dislocation loop core can be replaced by a charged sphere that creates an equivalent electrostatic capacity.[17] The inner cut-off radius of the equivalent spherical sink is

$$r_1^{(j)} = \pi(R_j^2 - r_d^2)^{1/2}/\ln(8R_j/r_d) \quad , \qquad j = 1,2 \quad . \tag{17}$$

The capture radius of small loops is obtained by putting $r_1^{(j)}$ from Ea. (17) into either Eq. (14) or Eqs. (15). The effective capture radius, $r_{v,i}^{(j)}$, or the preference factor, $\delta_{v,i}^{(j)}$, for small dislocation loops ($j = 1,2$) was calculated based on the infinitesimal loop approximation.[11,13,18] The effect of defect-loop interaction on defect flux is independent of the character of a dislocation loop as far as the first-order size interaction is concerned.[11] Therefore, $\delta_v^{(1)} = \delta_v^{(2)}$ and $\delta_i^{(1)} = \delta_i^{(2)}$ for both vacancy type and interstitial type of Frank loops.

When dislocation loops are large compared to the sphere of influence, the dislocation loops may be best approximated as straight dislocations of the lengths equal to their circumferences by using the relationship that the corresponding dislocation line density is

$$L_j = 2\pi R_j N_j \ , \qquad j = 1,2 \ , \tag{18}$$

where N_j is the number density of dislocation loops. In this approximation, the growth rates of dislocation loops are given by Eqs. (5) and (6).

2.2 Point Defect Concentrations

The point defect concentrations, $C_{v,i} = C_{v,i}(x,t)$, must satisfy the following defect conservation rate equations:

$$\frac{\partial C_v}{\partial t} = \frac{\partial}{\partial x}\left(D_v \frac{\partial C_v}{\partial x}\right) + G_v - \bar{R} C_v C_i - K_v C_v \ , \tag{19a}$$

$$\frac{\partial C_i}{\partial t} = \frac{\partial}{\partial x}\left(D_i \frac{\partial C_i}{\partial x}\right) + G_i - \bar{R} C_v C_i - K_i C_i \ , \tag{19b}$$

where $G_{v,i}$ are the point defect generation rates, $\bar{R}$ the mutual recombination constant, and $K_{v,i}$ are the reaction rate constants for point defects with the continuum sinks of all types.

2.2.1 Boundary Effects

The first term on the right-hand side of each of Eqs. (19) accounts for the diffusional loss of point defects to the reference boundary. An expression for the drift term due to a defect-boundary interaction has been derived by taking full account of the non-linearity of the interaction energy,[14] but because of the short range nature of the interaction between a point defect and a surface or an interface, the resulting contribution

to the diffusional loss by the drift term is usually small at elevated temperatures. The drift terms is, therefore, not included in the present model. However, such a short-range effect can be introduced into Eqs. (19) if the change in the activation energy of defect migration, $E^m_{v,i}$, near the boundary is known, e.g.,

$$E^m_{v,i} = E^m_{v,i}(x) \quad , \tag{20a}$$

$$D_{v,i} = D_{v,i}(x) = D^o_{v,i} \exp(-E^m_{v,i}/k_B T) \quad , \tag{20b}$$

where $D^o_{v,i}$ are the pre-exponential diffusion coefficients.

2.2.2 Recombination Rate

The rate constant for point defect annihilation by uncorrelated recombination, $\overline{R}$, depends on the probability that the faster interstitials will encounter vacancies in their diffusive movements, and is given by[19]

$$\overline{R} = 4\pi r_{vi}(D_i + D_v)/\Omega \quad , \tag{21}$$

where r_{vi} is the effective capture radius of a vacancy for interstitials or the radius of recombination volume. Based on the first-order cubic elastic anisotropy and the first-order size interaction, Yoo and Butler[11] and Schroeder and Dettman[20] have made theoretical analyses of how r_{vi} depends on the interaction strength, the inner cut-off radius, and temperature. The recombination rate constant used in the present work is based on Eq. (21) and the calculated recombination volume by our earlier work.[11]

2.2.3 Sink Strengths

The reaction rate constants for internal sinks are simply related to the so-called 'sink strength'[6,14,15] by

$$K_{v,i} = D_{v,i} k_{v,i}^2 , \tag{22}$$

and to a first approximation the total sink strength may be expressed as the sum of all the sink strengths by

$$k_v^2 = Z_v L + \sum_j 4\pi r_v^{(j)} N_j , \tag{23a}$$

$$k_i^2 = Z_i L + \sum_j 4\pi r_i^{(j)} N_j . \tag{23b}$$

If the loops are small, the summation includes $j = 1,2$ and $L = L_4$; whereas if the loops are large, the summation does not include $j = 1,2$ but $L = L_1 + L_2 + L_4$ as discussed previously. The approximation of the sink strength given by Eqs. (23) ignores the influence of one sink type on another type.

An exact description of the sink strength is perhaps the most important input and remains as the most demanding task in so far as theoretical modeling of radiation damage is concerned. This is a difficult task even for the steady state condition because of many sink effects. As for the combined sink strength of voids and dislocations, Brailsford et al.[15] have recently derived a transcendental equation for k (omitting the subscripts v or i),

$$k^2 = 4\pi r_1 N(1 + k r_1) + Z(k)L , \tag{24}$$

where r_1 and N are the radius and the number density of voids, respectively. An expression of Z(k) and the approximations of it for special cases are given in their paper.[15] The sink strength is time dependent as defect clusters grow and dislocation microstructure evolves during irradiation. Evolution of faulted loop microstructure results due mainly to the fact

that certain internal sinks have net fluxes of one point defect type over the other, i.e., $r_v^{(j)} \neq r_i^{(j)}$ and partly to the mutual interaction between sinks. After unfaulting, dislocation loops are transformed into a tangled microstructure. As dislocations climb under irradiation and interact with themselves to develop a cell structure, the cell boundaries can be treated as discrete interface boundaries. If solution treatment and/or cold working is applied prior to irradiation to create fine grain or cell sizes in the specimen, then a typical grain or cell may be treated as a bounded medium.

We are of the opinion that the rate theory model presented here and a quantitative analysis of microstructures by transmission electron microscopy (TEM) together can give the best estimates of sink strengths and 'sink efficiencies'.[21] Our preliminary result on the determination of the sink efficiency of faulted Frank loops in nickel during HVEM irradiation was reported in the recent conference.[22] In the example calculation that follows, the sink strengths are described by Eqs. (23) together with Eqs. (13)—(18).

2.2.4 Defect Generation Rate

Atomic displacement rate by fast electrons may be obtained from the experimentally measured electron flux, a threshold displacement energy, and the well documented data of displacement cross-sections.[23] In the case of ion bombardment, the various energy loss mechanisms have been developed,[2] and numerical methods now exist for calculating the depth distribution of atomic displacement rate.[24,25]

The point defect generation rate is lower than the atomic displacement rate, $\overline{G} = \overline{G}(x,t)$, by a substantial fraction because of correlated recombination and also defect clustering and annealing within the cascade regions in the case of heavy-ion bombardment. We are not certain as to what this fraction is for a given irradiation condition; but pending an exact treatment of this factor, f, we will assume that the depth variation

of the point defect generation rate has the same form as that of $\overline{G}$. The emission rate of thermal vacancies from dislocations and that from all the spherical sink types are, respectively,

$$G_v^L = Z_v L C_v^e \quad , \tag{25}$$

and

$$G_v^N = 4\pi \sum_j r_v^{(j)} N_j \overline{C}_j \quad , \tag{26}$$

where $j = 1,2,3$ for small loops and $j = 3$, $L = L_1 + L_2 + L_4$ for large loops. The total point defect generation rates are then given by

$$G_v = f\overline{G} + G_v^L + G_v^N \ , \tag{27a}$$

$$G_i = f\overline{G} \quad . \tag{27b}$$

As internal sinks evolve during irradiation the thermal emission contribution to the vacancy generation rate, Eq. (27a), is also dependent on spatial position. In order to include the effect of nucleation of small vacancy clusters from displacement cascades, one should introduce into Eqs. (27) two numerical factors such that more free interstitials are generated from displacement cascades than free vacancies, $f_i > f_v$, and the corresponding size and number density of vacancy clusters are continuously introduced into the sink terms, Eqs. (23). Straalsund[26] and Bullough et al.[7] found that the effect of such vacancy clusters on the correlation analyses of void swelling data by neutron and charged particles irradiation was a significant factor. This effect is not included, however, in the present example calculations.

Any time dependence of the point defect generation rate due to pulsed operation of reactors, as in some of the advanced concepts of fusion reactors,[27] can be explicitly put in Eqs. (19). Simulations of

recovery upon stopping irradiation and post-irradiation annealing of the microstructural radiation damage may also be modeled.

3. SOLUTION OF THE RATE EQUATIONS

3.1 Initial and Boundary Conditions

To solve the system of rate equations, Eqs. (2), (3), (4), and (19) or Eqs. (2), (5), (6), and (19), the initial and boundary conditions must be specified for ρ_1, ρ_2, ρ_3, C_v, and C_i. The initial conditions for point defects are

$$C_v(x,0) = C_v^e \ , \tag{28a}$$

$$C_i(x,0) = 0 \ . \tag{28b}$$

The initial conditions for the defect clusters are set to be a uniform distribution of small clusters having radii of a number multiple of Burgers vectors

$$\rho_j(x,0) = \overline{\rho}_j \ , \tag{29}$$

and these are subjected to a point defect conservation by

$$N_1\overline{\rho}_1^2 = N_2\overline{\rho}_2^2 + \frac{4}{3}N_3\overline{\rho}_3^3 \ . \tag{30}$$

Since the present model does not include the nucleation processes of the defect clusters, additional initial conditions on N_j and L are provided.

For the case of a semi-infinite medium with a free surface as the boundary, the boundary conditions are

$$C_v(0,t) = C_v^e \ , \qquad \lim_{x\to\infty} C_v(x,t) = C_v^e \ , \tag{31a}$$

$$C_i(0,t) = 0 \ , \qquad \lim_{x\to\infty} C_i(x,t) = 0 \ . \tag{31b}$$

For a foil of thickness d the boundary conditions at the mid-foil are

$$\frac{\partial C_v}{\partial x}(\frac{d}{2},t) = 0 \ , \tag{32a}$$

$$\frac{\partial C_i}{\partial x}(\frac{d}{2}, t) = 0 \ , \tag{32b}$$

while the same boundary conditions as before, Eqs. (31), apply at the surface x = 0.

3.2 Numerical Solutions

The system of rate equations subject to the initial and boundary conditions is solved numerically by a procedure known as the method of lines and by the stiff integrator package called GEAR-B.[28] First of all, a number, M + 1, of one-dimensional grid is chosen. The partial derivatives in x in Eqs. (19) are replaced by the finite difference quotients for defect concentrations on grid points, x_ℓ, $\ell = 1,2,\ldots\ldots,$ M + 1, where $x_1 = 0$ is taken as the free surface and x_{M+1} as the center of a foil or a large distance from the surface in the case of a semi-infinite medium (see Appendix A). The system of partial differential rate equations, Eqs. (2), (3), (4), and (19) or Eqs. (2), (5), (6), and (19), are cast into a vector form as was done by Myers et al.[29]

$$\dot{\underset{\sim}{Y}}(t) = \underset{\sim}{F}[Y(t),t] \ , \tag{33}$$

by assigning Y_1 as $C_v(x_1,t)$, Y_2 as $C_i(x_1,t)$, Y_3 as $\rho_1(x_1,t)$, Y_4 as $\rho_2(x_1,t)$, Y_5 as $\rho_3(x_1,t)$, Y_6 as $C_v(x_2,t)$, Y_7 as $C_i(x_2,t)$, Y_8 as $\rho_1(x_2,t)$, etc. (See Appendix A). This system of 5(M + 1) first-order ordinary differential equations is solved numerically subject to the initial conditions,

$$\underset{\sim}{Y}(0) = \overline{\underset{\sim}{Y}} \tag{34}$$

obtained from Eqs. (28) and (29). The boundary conditions of Eqs. (31) and (32) are incorporated into Eq. (33) (see Appendix A).

The present problem in the form of Eq. (33) has the property of stiffness due to the fact that some solutions decay at very different rate compared to others. In additions, the Jacobian matrix $(\partial\dot{Y}_i/\partial Y_j)$ in the present model is banded about its main diagonal with 5 non-zero diagonals above and 5 below. The stiff integrator GEAR-B developed by Hindmarsh[28] is designed to handle such problems. The governing equations developed so far (Appendix A) have been written into a FORTRAN program, from which the GEAR-B package is called. The computer program and typical outputs are listed in Appendices B and C, respectively.

4. EXAMPLE CALCULATIONS

An example problem is taken of 4 MeV $^{58}Ni^{2+}$ ion bombardment on a high-purity nickel semi-infinite medium at T = 823 K (550°C). The deposition of initial damage energy was calculated by using the computer program E-DEP-1[24] with the nickel density of $\rho_0 = 9.13 \times 10^{22}$ cm^{-3} and the electronic stopping power parameter of $k_e = 0.162$. This was converted to the atomic displacement rate by the modified Kinchin and Pease formula[30] and an estimate of ion flux at the peak position, $\phi = 1$ μA/cm^2.[31] In Fig. 1 the calculated atomic displacement rate, $\overline{G}$, is plotted with respect to the ion penetration depth. The rate of point defects escaping the cascade regions is assumed to be $f\overline{G}$ with f = 0.2.

The problem is set up by M = 26 increments of varying sizes between $x_1 = 0$ and $x_{27} = 4.8$ μm. Vacancy loops survive for a relatively short

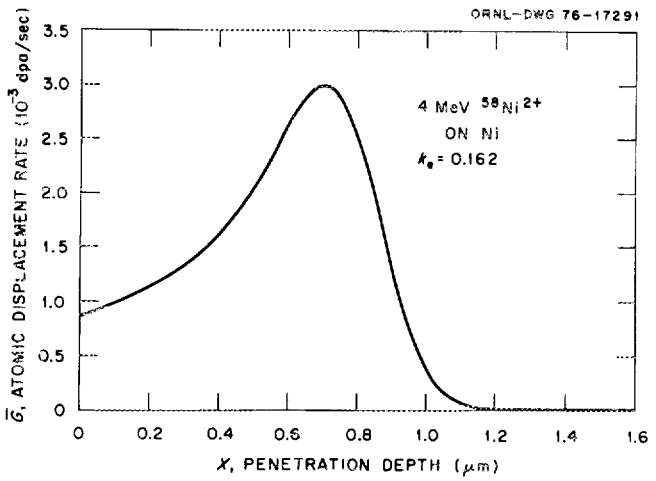

Fig. 1. Atomic Displacement Rate Approximated from the Energy Deposition of Initial Damage Energy Calculated by E-DEP-1.

time, and these are neglected in the present calculation. Therefore, a total of $4(M + 1) = 108$ rate equations are integrated. The diffusion coefficients are assumed to be independent of position. The material and defect parameters used for the calculations are given in Table 1.

4.1 Recombination Dominant Case

This limiting case is attained by setting the reaction rate constants to zero, $K_v = K_i = 0$. Calculated vacancy diffusion profiles, $D_v(C_v + C_v^e)$, are plotted in Fig. 2. They start from the initial value, $D_v C_v^e$, and rise gradually into a stationary profile. In the case of interstitials, however, there appears a transient surge of diffusion profiles, $D_i C_i$, roughly over $t = 10^{-6} \sim 10^{-3}$ sec range as shown in Fig. 3. The difference between the two, $D_i C_i - D_v(C_v + C_v^e)$, may be considered as the 'defect diffusion potential' for nucleation of interstitial clusters. This is plotted in Fig. 4. for the peak position, $x = 0.7$ μm, with respect to irradiation time. Far from the surface with no internal sinks, one obtains for a steady state the following:

$$D_v C_v = D_i C_i = \left(\frac{G\Omega D_v}{4\pi r_{vi}}\right)^{1/2} , \qquad (35)$$

Table 1. Materials Constants and Defect Parameters for Ni

$\mu = 9.5 \times 10^{10}$ Pa	$\nu = 0.28$
$a = 3.52$ Å	$b = a/\sqrt{3}$
$r_{vi}/a = 1.2$	$r_d/b = 2$
$\gamma = 0.4$ J/m^2	$\Gamma = 1$ J/m^2
$E_v^f = 1.6$ eV	$S_v^f/k_B = 1.5$
$E_v^m = 1.2$ eV	$D_v^o = 0.19$ cm^2/sec
$E_i^m = 0.15$ eV	$D_i^o = 0.008$ cm^2/sec

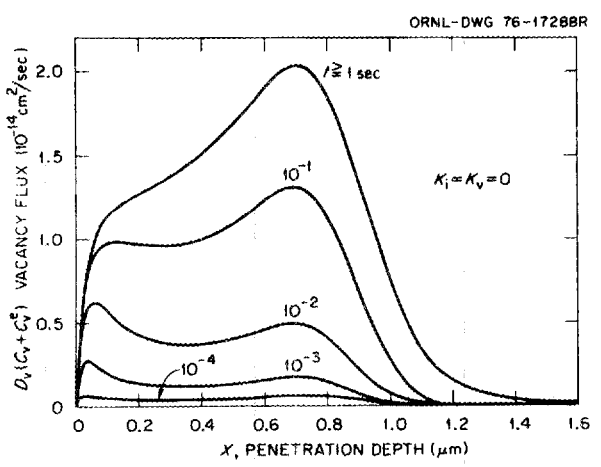

Fig. 2. Vacancy Diffusion Profiles for the Recombination Dominant Case.

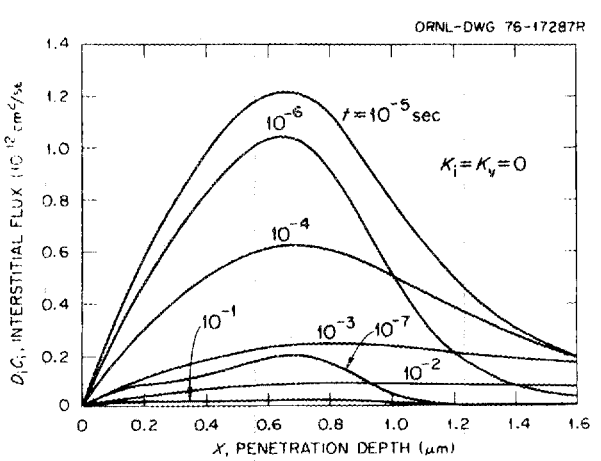

Fig. 3. Interstitial Diffusion Profiles for the Recombinaion Dominant Case

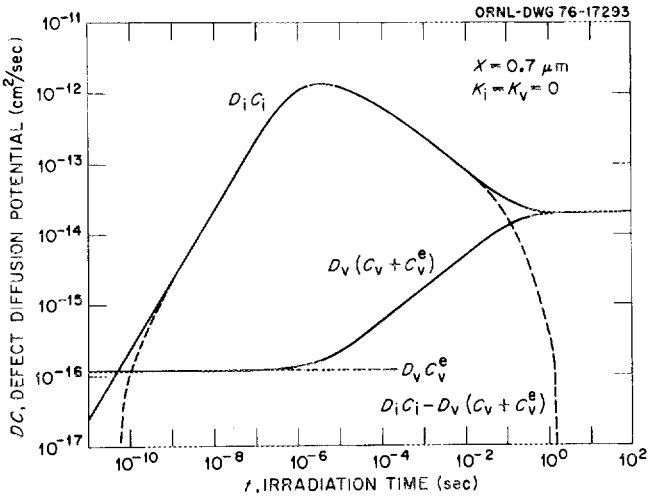

Fig. 4. Defect Diffusion Potentials at the Peak Position for the Recombination Dominant Case.

with which G at x = 0.7 μm yields a value of 2.06×10^{-14} cm^2/sec. The calculated steady state value at the peak position (Fig. 4.) is 2.04×10^{-14} cm^2/sec, which is 0.9% smaller than the infinite medium value. It can be inferred from Fig. 4. that if there were no internal sinks at the start of irradiation, interstitial clusters such as interstitial dislocation loops may nucleate within $t < 1$ sec.

4.2 Sink Dominant Case

As for the other extreme situation we consider a sink dominant case where there is no recombination, $\overline{R} = 0$, and the internal sinks consist of dislocations of $L = 10^{11}$ cm^{-2} with $\delta_v = 0$ and $\delta_i = 0.1$. Equations (19a) and (19b) are then decoupled from one another. The mean free paths of point defects before annihilating at dislocations are $k_v^{-1} = 245$ Å and $k_i^{-1} = 242$ Å. Calculated defect diffusion profiels are shown in Figs. 5 and 6. The transient surge of interstitial diffusion profile in this case (Fig. 6) is much less pronounced than in the recombination dominant case (Fig. 3). The transience of defect diffusion potentials at the peak position is shown in Fig. 7. The steady state values for an infinite medium in this case are given by

$$\left(D_v C_v\right)^{\infty} = G_i / Z_v L \ , \tag{36a}$$

$$\left(D_i C_i\right)^{\infty} = G_i / Z_i L \ , \tag{36b}$$

where thermal vacancies are neglected. The calculated steady state values (Fig.7) are 1.43×10^{-14} cm^2/sec and 1.38×10^{-14} cm^2/sec for vacancies and interstitials, respectively, which are 0.9% and 1.7% smaller than the corresponding values calculated by Eqs. (36). Insofar as the role the net point defect flux plays in the processes of defect clustering, the results of Fig. 7 may be interpreted as follows: under the constant sink strengths of $k_i^2 = 1.70 \times 10^{11}$ cm^{-2} and $k_v^2 = 1.66 \times 10^{11}$ cm^{-2} interstitial dislocation loops may nucleate before $t = 10^{-3}$ sec, whereas vacancy type clusters may nucleate after $t = 10^{-3}$ sec.

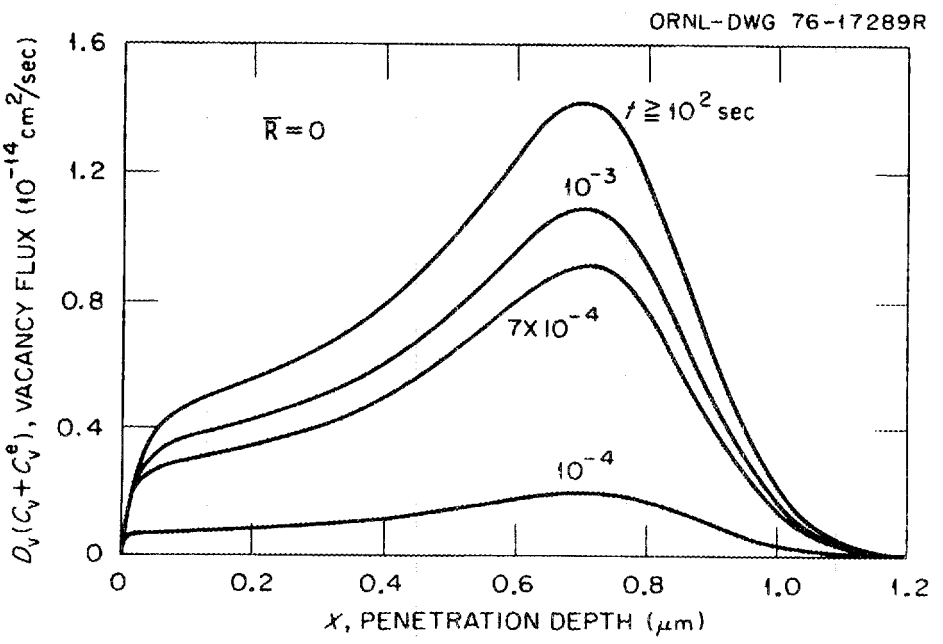

Fig. 5. Vacancy Diffusion Profiles for the Sink Dominant Case with $L = 10^{11}$ cm^{-2}, $\delta_v = 0$, $\delta_i = 0.1$.

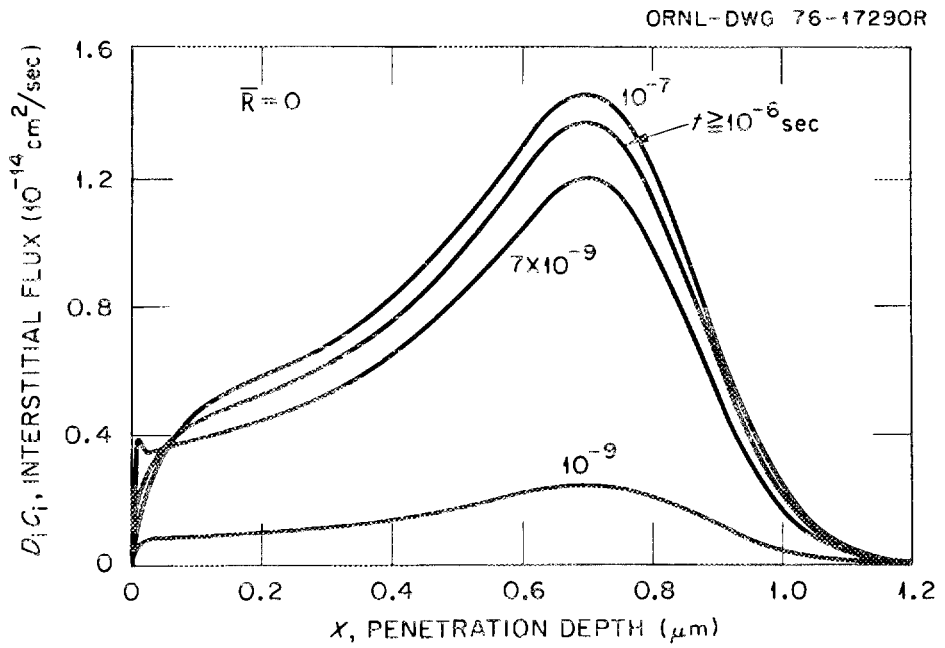

Fig. 6. Interstitial Diffusion Profiles for the Sink Dominant Case with $L = 10^{11}$ cm^{-2}, $\delta_v = 0$, $\delta_i = 0.1$.

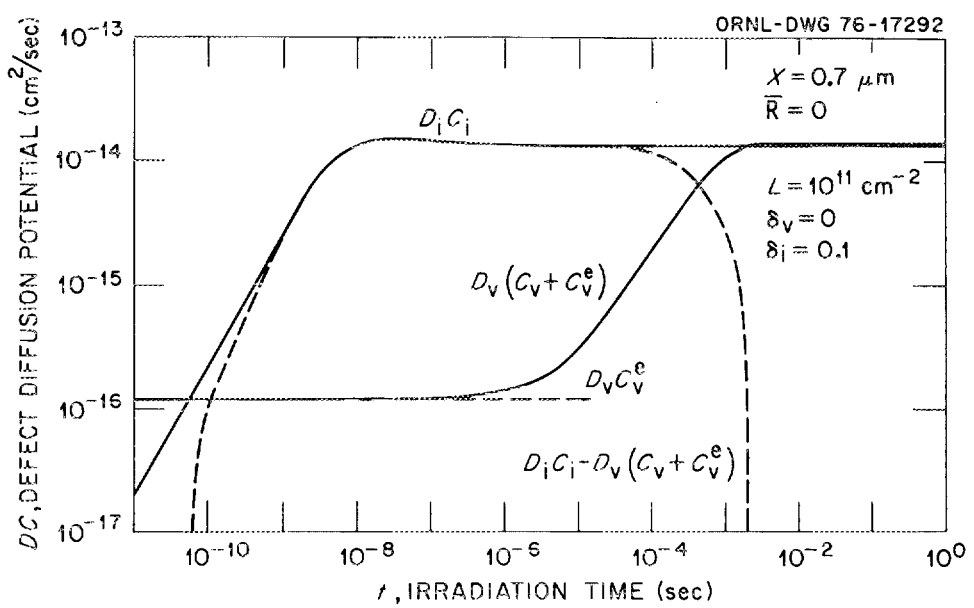

Fig. 7. Defect Diffusion Potentials at the Peak Position for the Sink Dominant Case.

4.3 General Case

The following sink densities are chosen for the calculation: $N_1 = 4 \times 10^{14}$ cm^{-3}, $N_3 = 2 \times 10^{14}$ cm^{-3}, $L = 1 \times 10^{10}$ cm^{-2}. These are held constant with respect to both time and position. Given an initial size of voids, e.g., $\overline{\rho}_3 = 5$, the initial radius of interstitial loops was set by

$$\overline{\rho}_1 = \left[\frac{4}{3}\left(\frac{N_3}{N_1}\right)\overline{\rho}_3^3\right]^{1/2} \quad . \tag{37}$$

Initially (t = 0), the cavities of radius, $R_3 = \overline{\rho}_3 b$, are assumed to be small equilibrium gas bubbles containing n_g gas atoms, Eq. (12). Then, with the constant n_g, P_g decreases as R_3 increases as expressed by Eq. (11) thus characterizing the growing voids. The growth rate of interstitial loops given by Eqs. (5), (7), and (16) is used with $\delta_v^{(4)} = 0$ and $\delta_i^{(4)} = 0.6$. It is assumed that the loops unfault with their radius exceed their sphere of influence, $R_s = 421$ b. The interaction between a point defect and a void may be incorporated into the present model by setting appropriate non-zero values for preference factors, $\delta_v^{(3)} \neq \delta_i^{(3)}$.[32,33] However, because of the relatively weak strength of the preference factors as compared to those for dislocations and dislocation loops, we assume that voids are weak neutral sinks, i.e., $\delta_v^{(3)} = \delta_i^{(3)} = 0$.

The time dependences of the defect diffusion potentials and the loop and void radii at the peak position, x = 0.7 μm, are shown in Fig. 8. Interstitial loops grow continuously, and after t = 100 sec the growth rate increases to show an exponent of approximately n = 0.9 for $(R_1/b)\alpha t^n$. Whereas, voids shrink slightly until $t = 10^{-2}$ sec at which $D_v(C_v + C_v^e)$ and $D_i C_i$ cross over. Beyond this time the void growth rate steadily increases to reach n = 0.5 for $(R_3/b)\alpha t^n$ at $t > 10^2$ sec. Void swelling of a specimen of volume V is

$$S = \frac{\Delta V}{V - \Delta V} \quad , \tag{38a}$$

$$\frac{\Delta V}{V} = \frac{4}{3}\pi R_3^3 N_3 \quad . \tag{38b}$$

The time dependent void swelling at x = 0.7 μm is shown in Fig. 9. The time exponent of n = 1.4 for $S\alpha t^n$ is obtained toward the end of irradiation time to the dose of 1 dpa. The rate of approach to this dose dependence of void swelling depends directly on the chosen initial value of void size as illustrated in Fig. 9.

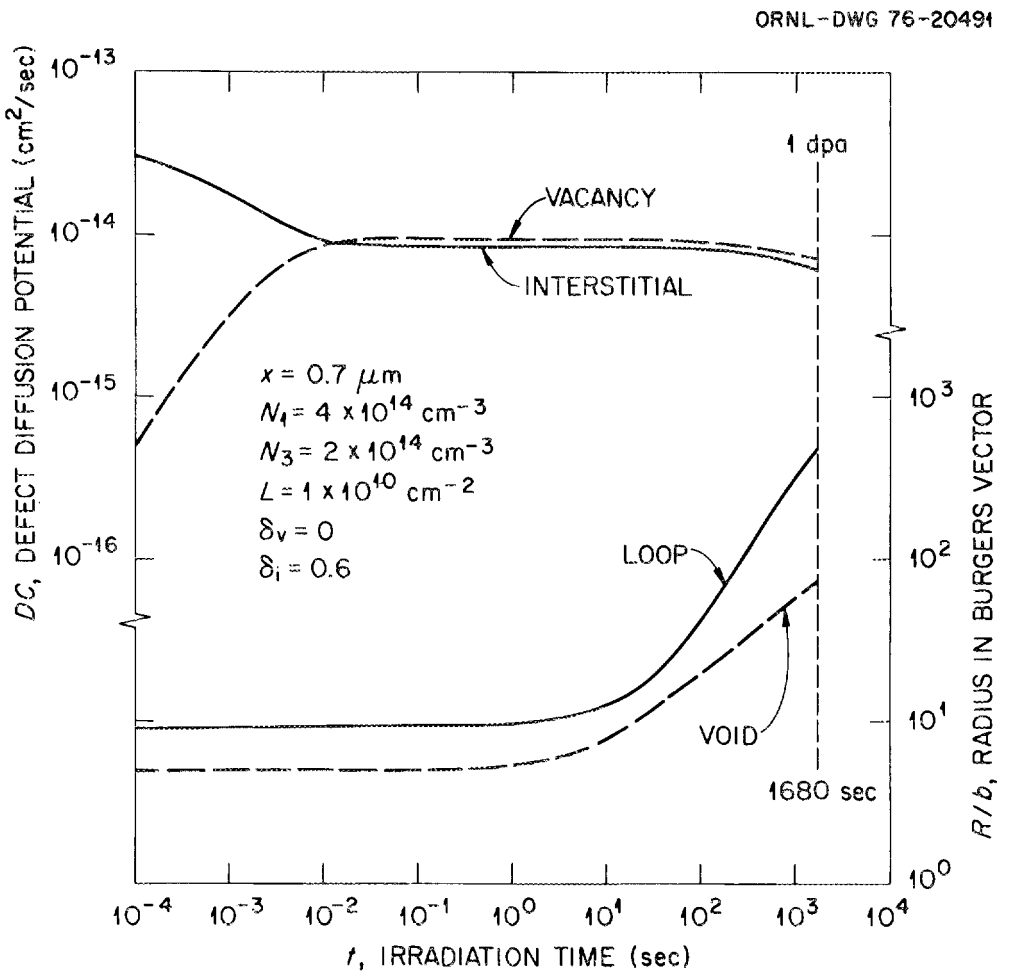

Fig. 8. Defect Diffusion Potentials and Interstitial Loop and Void Radii at the Peak Position.

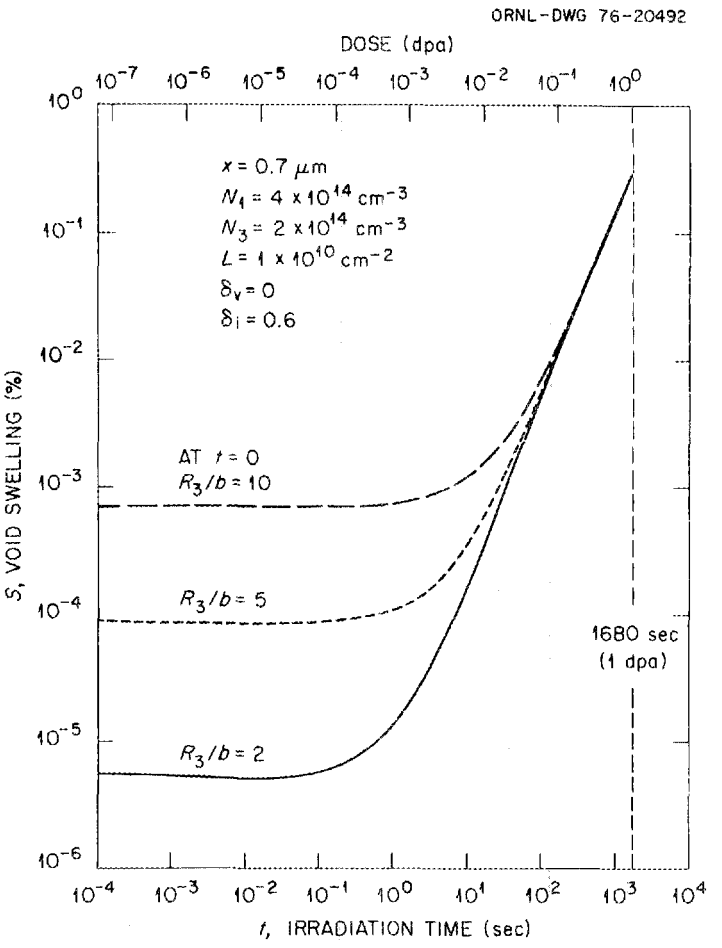

Fig. 9. Void Swelling Rates for Three Initial Conditions.

The spatial dependences of the defect concentrations and the loop and void radii at t = 1680 sec are shown in Fig. 10. The shape of the depth profile of vacancy concentration is the same as that of interstitial concentration as shown in Fig. 10(a). Two peaks of loop radius appear in Fig. 10(b), R_1 = 502b at x = 0.04 μm and R_1 = 484b at x = 0.74 μm. As unfaulted loops, large loops at these depths grow into the dislocation microstructure. Since the front peak position is only 400 Å from the free surface, a portion of each loop must intersect the surface. If an interstitial loop were to stop growing upon intersecting the surface, then a smaller peak near the surface would result as approximated by

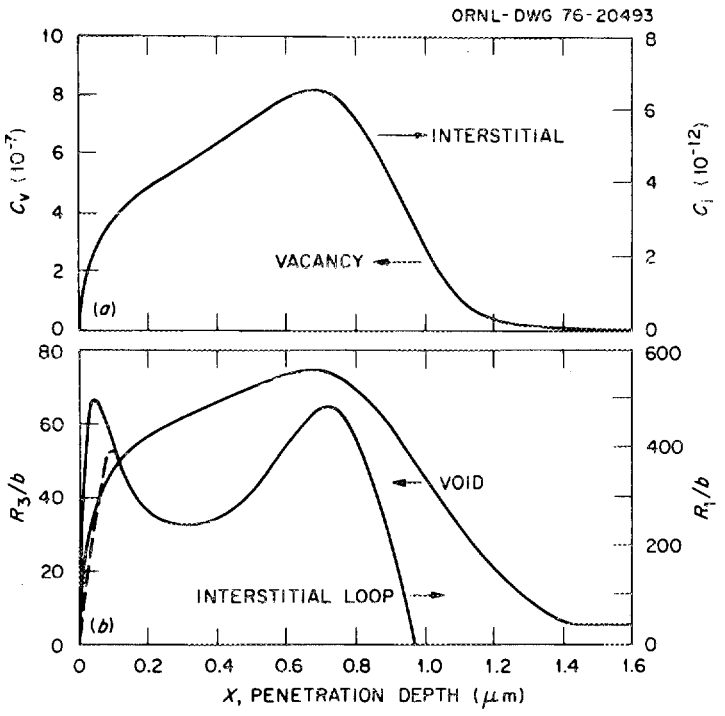

Fig. 10. Depth Profiles of Vacancy and Interstitial Concentrations and Interstitial Loop and Void Radii at t = 1680 sec.

the dashed curve in Fig. 10(b). The depth profile of void radius is also shown in Fig. 10(b). Table 2 shows the calculated values of G, the sink strength, the loop and void radii, and the swelling for three reference depth positions. Even though the irradiation dose at the front position (x = 0.14 μm) is 6% higher than that at the back (x = 0.92 μm), the void swelling at the front is 23% lower than at the back. The reason for this is the proximity effect of the free surface.

5. SUMMARY AND DISCUSSION

A system of partial differential rate equations for vacancies, self-interstitials, dislocation loops and voids in one-dimensionally bounded media, viz. a thin foil and a semi-infinite medium, under charged particle irradiation has been formulated in terms of diffusion controlled kinetics of defect annealing and clustering. The rate equations are

Table 2. Numerical Results at Three Reference Positions

	Front	Peak	Back
x(μm)	0.14	0.70	0.92
G(10^{-4} dpa/sec)	2.10	6.00	1.95
dose (dpa)	0.35	1.01	0.33
k_v^2 (10^{10} cm^{-2})	3.69	4.81	2.72
k_i^2 (10^{10} cm^{-2})	4.05	5.28	2.98
R_1/b	328.	483.	177.
R_3/b	52.	74.	56.
S (%)	0.10	0.29	0.13

integrated numerically to give the growth rate of interstitial loops and the void swelling rate. An example calculation for 4 MeV Ni self-ion bombardment on a semi-infinite medium at 550°C gives the following summary: (a) While the loops grow continuously, the voids initially shrink ($t < 10^{-2}$ sec) before starting to grow. This is because of the transient net flux of faster interstitials, $D_i >> D_v$. (b) At the low dose range of less than 0.1 dpa, the void swelling rate depends directly on the initial size of voids chosen for the calculation. (c) Two peaks, one near the free surface and another near the peak damage position, appear on the depth variation of loop size. The peak near the surface arises because of the proximity of the free surface as a neutral sink and the high perference factor of dislocations for interstitials, $\delta_i^{(4)} = 0.6$, $\delta_b^{(4)} = 0$. (d) Because of the free surface, the void swelling near the surface is lower than at a reference position far away from the surface even when the defect generation rate and the total dose near the surface are greater than those at the reference position. (e) If there were no internal sinks initially, e.g., a single crystal semi-infinite medium with a low dislocation density, interstitial clusters such as interstitial loops may nucleate within $t < 1$ sec. (f) If a specimen initially contains a high density of stable dislocations ($L = 1 \times 10^{11}$ cm^{-2}) as in cold-worked metal, then the nucleation of

interstitial loops may take place within $t < 10^{-3}$ sec, whereas vacancy clusters may nucleate beyond $t > 10^{-3}$ sec.

Many applications of the present model are possible, e.g., microstructural damage recovery, post-irradiation annealing, pulsed irradiation, stress effects, gas bubble growth, etc. The computer execution time to obtain the results of Figs. 8, 9, and 10 was only about 2 minutes. Therefore, a future extension of the present model to include more mobile defects and internal sinks is promising. The most important unsolved problem, however, is the characterization of the collective sink strength of an evolving microstructure of internal sinks of various types. In our opinion, this can be best solved by quantitative analyses of TEM microstructures by use of the rate theory model presented here.

REFERENCES

1. *Radiation Effects and Tritium Technology for Fusion Reactors*, ed. by J. S. Watson and F. W. Wiffen, Proceedings of the International Conference held at Gatlinburg, Tenn., Oct. 1–3, 1975, CONF-750989, 1976.
2. *Fundamental Aspects of Radiation Damage in Metals*, ed. by M. T. Robinson and F. W. Young, Jr., Proceedings of the International Conference held at Gatlinburg, Tenn., Oct. 6–10, 1975, CONF-751006, 1975.
3. *Correlation of Neutron and Charged Particles Damage*, Proceedings of the Workshop held at Oak Ridge, Tenn., June 8–9, 1976.
4. S. D. Harkness and Che-Yu Li, *Metall. Trans.* 2, 1457 (1971).
5. H. Wiedersich, *Rad. Effects* 12: 111 (1972).
6. A. D. Brailsford and R. Bullough, *J. Nucl. Mater.* 44: 121 (1972).
7. R. Bullough, B. L. Eyre, and K. Kirshan, *Proc. R. Soc. Lond. A.* 346: 81 (1975).
8. F. A. Garner and G. L. Guthrie, "The Influence of Displacement Gradients on the Interpretation of Charged Particle Simulation Experiments," p. I-491 in *Radiation Effects and Tritium Technology for Fusion Reactors*, ed. by J. S. Watson and F. W. Wiffen, Proceedings of the International Conference held at Gatlinburg, Tenn., Oct 1–3, 1975, CONF-750989, 1976.

9. E. J. Savino, *Void Swelling in Thin Foils*, Harwell Report, AERE-TP-610 (July 1975).

10. N. Ghoniem and G. Kulcinski, "Void Growth Kinetics under Pulsed Irradiation," Proceedings of the International Conference on *The Properties of Atomic Defects in Metals*, Argonne, Ill., Oct. 18–22, 1976, (to be published in *Journal of Nuclear Materials)*.

11. M. H. Yoo and W. H. Butler, *Phys. Stat. Sol.* B77: 181 (1976).

12. F. S. Ham, *J. Appl. Phys.* 30: 915 (1959).

13. M. H. Yoo, W. H. Butler, and L. K. Mansur, "Defect Annealing and Clustering in the Elastic Interaction Force Field," Vol. 2, p. 804 in *Fundamental Aspects of Radiation Damage in Metals*, ed. by M. T. Robinson and F. W. Young, Jr., Proceedings of the International Conference held at Gatlinburg, Tenn., Oct 6–10, 1975, CONF-751006, 1975.

14. M. H. Yoo and L. K. Mansur, *J. Nucl. Mater.* 62: 282 (1976).

15. A. D. Brailsford, R. Bullough, and M. R. Hayns, *J. Nucl. Mater.* 60: 246 (1976).

16. I. G. Margvelashvili and Z. K. Saralidze, *Sov. Phys.: Solid St.* 15: 1774 (1974).

17. C. P. Flynn, *Point Defects and Diffusion*, Clarendon Press, Oxford p. 486 (1972).

18. W. G. Wolfer and M. Ashkin, *J. Appl. Phys.*46: 547 (1975).

19. T. R. Waite, *Phys. Rev.* 107: 463 (1957).

20. K. Schroeder and K. Dettmann, *Z. Physik* B22: 343 (1975).

21. R. W. Balluffi, "Voids, Dislocation Loops and Grain Boundaries as Sinks for Point Defects," Vol. 2, p. 852 in *Fundamental Aspects of Radiation Damage in Metals*, ed. by M. T. Robinson and F. W. Young, Jr., Proceedings of the International Conference held at Gatlinburg, Tenn., Oct. 6–10, 1975, CONF-751006, 1975.

22. M. H. Yoo and J. O. Stiegler, "Point Defect Interactions and Growth of Dislocation Loops," Proceedings of the International Conference on *The Properties of Atomic Defects in Metals*, Argonne, Ill., Oct. 18–22, 1976 (to be published in *Journal of Nuclear Materials)*.

23. O. S. Oen, "Cross Sections for Atomic Displacements in Solids by Fast Electrons," Oak Ridge Report, ORNL-4897 (August 1973).

24. I. Manning and G. P. Mueller, *Comput. Phys. Commun.* 7: 85 (1974).

25. D. K. Brice, *Ion Implantation Range and Energy Deposition Distributions*, Vol. 1, Plenum Press, New York, 1975.

26. J. L. Straalsund, *J. Nucl. Mater.* 51: 302 (1974).

27. J. O. Schiffgens, N. J. Graves, and D. G. Doran, "An Analysis of Irradiation with Time-Dependent Sources," p. I-532 in *Radiation Effects and Tritium Technology for Fusion Reactors*, ed. by J. S. Watson and F. W. Wiffen, Proceedings of the International Conference held at Gatlinburg, Tenn., Oct. 1–3, 1975, CONF-750989, 1976.

28. A. C. Hindmarsh, *GEAR-B: Solution of Ordinary Differential Equations Having Banded Jacobians*, Lawrence Livermore Laboratory Report UCID-30059, Rev. 1 (March 1975).

29. S. M. Myers, D. E. Amos, and D. K. Brice, *J. Appl. Phys.* 47: 1812 (1976).

30. I. M. Torrens and M. T. Robinson, "Computer Simulation of Atomic Displacement Cascades in Metals," *Radiation Induced Voids in Metals*, ed. by J. W. Corbett and L. C. Ianniello, ERDA CONF-71060, 1972.

31. N. H. Packan, J. O. Stiegler, and K. Farrell, "Correlation of Neutron and Nickel-Ion Radiation," to be published.

32. W. G. Wolfer, "Segragation of Point Defects by Internal Stress Fields," Vol. 2, p. 813 in *Fundamental Aspects of Radiation Damage in Metals*, ed. by M. T. Robinson and F. W. Young, Jr., Proceedings of the International Conference held at Gatlinburg, Tenn., Oct. 6–10, 1975, CONF-751006, 1975.

33. L. K. Mansur and W. G. Wolfer, "Influence of a Surface Coating on Void Formation," Proceedings of the International Conference on *The Properties of Atomic Defects in Metals*, Argonne, Ill., Oct. 18–22, 1976 (to be published in *Journal of Nuclear Materials*).

APPENDIX A

The second-order derivative of the defect concentration, C, with respect to the depth position, x, is expressed by the finite difference quotient,[29]

$$\frac{\partial}{\partial x}\left(D\frac{\partial C}{\partial x}\right) \simeq \left[D_{\ell+1/2}\left(\frac{C_{\ell+1} - C_{\ell}}{\Delta x_{\ell}}\right) - D_{\ell-1/2}\left(\frac{C_{\ell} - C_{\ell-1}}{\Delta x_{\ell-1}}\right)\right]\left(\frac{\Delta x_{\ell} + \Delta x_{\ell-1}}{2}\right)^{-1} \tag{A1}$$

$$\simeq \alpha_{\ell}C_{\ell-1} - \beta_{\ell}C_{\ell} + \gamma_{\ell}C_{\ell+1} \quad ,$$

where

$$\alpha_{\ell} = 2D_{\ell-1/2}/\Delta x_{\ell-1}(\Delta x_{\ell} + \Delta x_{\ell-1}) \quad , \tag{A2}$$

$$D_{\ell+1/2} = (D_{\ell+1} + D_{\ell})/2 \quad , \tag{A3}$$

$$\Delta x_{\ell} = x_{\ell+1} - x_{\ell} \quad , \tag{A4}$$

$$\gamma_{\ell} = 2D_{\ell+1/2}/\Delta x_{\ell}(\Delta x_{\ell} + \Delta x_{\ell-1}) \quad , \tag{A5}$$

$$\beta_{\ell} = \alpha_{\ell} + \gamma_{\ell} \quad . \tag{A6}$$

The above equations (A1–A6) replace diffusional flux terms in Eqs. (19).

The system of 5(M + 1) governing rate equations, Eq. (33), for a semi-infinite medium has the following general form:

$$\frac{dY_1}{dt} = \frac{dY_2}{dt} = \frac{dY_3}{dt} = \frac{dY_4}{dt} = \frac{dY_5}{dt} = 0 \quad , \tag{A7}$$

$$\frac{dY_{5\ell-4}}{dt} = \alpha_{\ell}^{v}Y_{5\ell-9} - \beta_{\ell}^{v}Y_{5\ell-4} + \gamma_{\ell}^{v}Y_{5\ell+1} + G_{\ell}^{v} - \overline{R}Y_{5\ell-4}Y_{5\ell-3} - K_{\ell}^{v}\,Y_{5\ell-4} \quad , \tag{A8-a}$$

$$\frac{dY_{5\ell-3}}{dt} = \alpha^i_\ell Y_{5\ell-8} - \beta^i_\ell Y_{5\ell-3} + \gamma^i_{5\ell+2} + G^i_\ell - \overline{R}Y_{5\ell-4}Y_{5\ell-3} - K^i_\ell Y_{5\ell-3} \quad , \tag{A8-b}$$

$$\frac{dY_{5M-4}}{dt} = \alpha^v_M Y_{5M-9} - \beta^v_M Y_{5M-4} + \gamma^v_M C^e_v + G^v_M - \overline{R}Y_{5M-4}Y_{5M-3} - K^v_M Y_{5M-4} \quad , \tag{A9-a}$$

$$\frac{dY_{5M-3}}{dt} = \alpha^i_M Y_{5M-8} - \beta^i_M Y_{5M-3} + G^i_M - \overline{R}Y_{5M-4}Y_{5M-3} - K^i_M Y_{5M-3} \quad , \tag{A9-b}$$

with the superscripts v and i for vacancies and interstitials and the subscripts $\ell = 2, 3, \ldots, M$. The boundary conditions, Eqs. (31), that $Y_{5M+1} = C^e_v$ and $Y_{5M+2} = 0$ have been used for the last two Eqs. (A9); for these boundary conditions to be realistic x_{M+1} must sufficiently exceed the range of point defect generation. For the sinks, ρ_j, Eqs. (2), (3), and (4) become

$$\frac{dY_{5\ell-2}}{dt} = 2\left[r^i_{5\ell-2}D^i_\ell Y_{5\ell-3} - r^v_{5\ell-2}D^v_\ell\left(Y_{5\ell-4} - \overline{C}^{(1)}_\ell\right)\right] / \left(Y_{5\ell-2}b^3\right) \quad , \tag{A10}$$

$$\frac{dY_{5\ell-1}}{dt} = 2\left[r^v_{5\ell-1}D^v_\ell\left(Y_{5\ell-4} - \overline{C}^{(2)}_\ell\right) - r^i_{5\ell-1}D^i_\ell Y_{5\ell-3}\right] / \left(Y_{5\ell-1}b^3\right) \quad , \tag{A11}$$

$$\frac{dY_{5\ell}}{dt} = \left[r^v_{5\ell}D^v_\ell\left(Y_{5\ell-4} - \overline{C}^{(3)}_\ell\right) - r^i_{5\ell}D^i_\ell Y_{5\ell-3}\right] / \left(Y^2_{5\ell}b^3\right) \quad , \tag{A12}$$

and Eqs. (5) and (6) become

$$\frac{dY_{5\ell-2}}{dt} = \left[Z^i D^i_\ell Y_{5\ell-3} - Z^v D^v_\ell \left(Y_{5\ell-4} - \bar{C}^{(1)}_\ell\right)\right] / b^2, \tag{A13}$$

$$\frac{dY_{5\ell-1}}{dt} = \left[Z^v D^v_\ell \left(Y_{5\ell-4} - \bar{C}^{(2)}_\ell\right) - Z^i D^i_\ell Y_{5\ell-3}\right] / b^2 \quad , \tag{A14}$$

where $\ell = 2, 3, \ldots, M + 1$.

For a foil problem, all the equations from (A7) to (A14) equally apply except that Eqs. (A9) must be replaced to satisfy the zero-flow boundary condition at the mid-foil, $x_{M+1} = d/2$, by the following:

$$\begin{aligned}\frac{dY_{5M+1}}{dt} = {} & \left(D^v_{M+1} + D^v_M\right)\left(Y_{5M-4} - Y_{5M+1}\right) / \left(\Delta x_M\right)^2 \\ & + G^v_{M+1} - \bar{R}Y_{5M+1}Y_{5M+2} - K^v_{M+1}\, Y_{5M+1} \quad ,\end{aligned} \tag{A15-a}$$

$$\begin{aligned}\frac{dY_{5M+2}}{dt} = {} & \left(D^i_{M+1} + D^i_M\right)\left(Y_{5M-3} - Y_{5M+2}\right) / \left(\Delta x_M\right)^2 \\ & + G^i_{M+1} - \bar{R}Y_{5M+1}Y_{5M+2} - K^i_{M+1}Y_{5M+2} \quad .\end{aligned} \tag{A15-b}$$

APPENDIX B

The main program is listed in this Appendix B. The input data cards for the deposition of damage energy, GP, were generated by simply punching out cards for SD form E-DEP-1. Subroutine DRIVEB of the GEAR-B package is called from this main program. A proper setting of appropriate dimensions in the subroutine DRIVEB is the only necessary adjustment to the GEAR-B package.

Also listed in this Appendix B are the two subroutines required by the GEAR-B package. First, in DIFFUN the governing differential rate equations are established in a vector form. Second, a dummy subroutine PDB is required even when the Jacobian matrix is evaluated numerically with the flag MF = 22.

Instructions on the usage of the GEAR-B package are given in the Lawrence Livermore Laboratory Report by Hindmarsch.[28] The computer code is available from the Argonne Code Center.

```
C
C  GROWTH KINETICS OF DEFECT CLUSTERS IN A SEMI-INFINITE MEDIUM
C  DURING HEAVY ION IRRADIATION
C
C     REFERENCE..A. C. HINDERMARSH, GEARB.. SOLUTION OF ORDINARY DIFFERENTIAL
C        EQUATIONS HAVING BANDED JACOBIAN, LAWRENCE LIVERMORE LABORATORY
C        REPORT UCID-30059, REV. 1, MARCH 1975
C
C  THIS MAIN PROGRAM CALLS SUBROUTINE DRIVEB
C  INPUT IS TAKEN ON LOGICAL UNIT LIN, WHICH IS SET EQUAL TO 5
C  OUTPUT IS WRITTEN ON LOGICAL UNIT LOUT, WHICH IS SET EQUAL TO 6
C
      IMPLICIT REAL*8 (A-H,O-Z)
      COMMON /GEAR9/ HUSED,NQUSED,NSTEP,NFE,NJE
      COMMON /GEARA/ R,O,BV,DV,DI,RCO,RVO,CVE,M
      COMMON /GEARB/ DN1,DN2,DN3,DL4,SBN,SE,SF,GN,BF
      COMMON /GEARC/ PI,AKT,BVS,RSL,ZV,ZI
      COMMON /GEARD/ SS1(27),SS2(27),ALP(27),BET(27),GAM(27),G(27)
      COMMON /GEARE/ C1(27),C3(27)
      DIMENSION Y0(108),CV(27),CI(27),R1(27),R3(27)
      DIMENSION GP(131),X(28),DX(27),DCD(27),TT(20)
      DATA LIN/5/,LOUT/6/
      DATA X/0.D0,0.01D0,0.02D0,0.04D0,0.08D0,0.14D0,0.22D0,0.32D0,
     A0.42D0,0.52D0,0.6D0,0.66D0,0.7D0,0.74D0,0.8D0,0.86D0,0.92D0,
     B0.98D0,1.04D0,1.1D0,1.16D0,1.24D0,1.4D0,1.7D0,2.2D0,3.1D0,4.8D0,
     C8.D0/
      DATA TT/1.D-4,1.D-3,1.D-2,1.D-1,1.D0,1.D+1,1.D+2,1.D+3,1.68D+3/
      PI=3.1415926535897932D0
      BC=0.86204744D-4
      BB=1.361D-16
      BF=1.7D-23
      EX3=1.D0/3.D0
C
C  INPUT PARAMETERS:
C  TM = TEMPERATURE (K)
C  A0 = LATTICE PARAMETER (CM)
C  R0 = RADIUS OF RECOMBINATION VOLUME (A0)
C  RCO = DISLOCATION CORE RADIUS (BV)
C  RVO = VOID CUT-OFF RADIUS (BV)
C  SM = SHEAR MODULUS (DYNES/CM2)
C  PR = POISSONS RATIO
C  SE = STACKING FAULT ENERGY (ERGS/CM2)
C  SF = SURFACE ENERGY (ERGS/CM2)
C  DOV = PRE-EXPONENTIAL DIFFUSION CONSTANT OF VACANCIES (CM2/SEC)
C  DOI = PRE-EXPONENTIAL DIFFUSION CONSTANT OF INTERSTITIALS (CM2/SEC)
C  EMV = MIGRATION ENERGY OF VACANCIES (EV)
C  EMI = MIGRATION ENERGY OF INTERSTITIALS (EV)
C  SFV = VACANCY FORMATION ENTROPY (BC)
C  EFV = VACANCY FORMATION ENTHALPY (EV)
C  DN1 = NUMBER DENSITY OF INTERSTITIAL TYPE LOOPS (1/CM3)
C  DN2 = NUMBER DENSITY OF VACANCY TYPE LOOPS (1/CM3)
C  DN3 = NUMBER DENSITY OF VOIDS (1/CM3)
C  DL4 = DISLOCATION LINE DENSITY (1/CM2)
C  DL4I = PREFERENCE FACTOR OF STRAIGHT DISLOCATIONS FOR INTERSTITIALS
C  G = DEFECT GENERATION RATE (DPA/SEC)
C
```

```
      READ(LIN,1) TM,A0,R0,RC0,RV0,DL4I
    1 FORMAT(8D10.0)
      READ(LIN,1) SM,PR,SE,SF
      READ(LIN,1) D0V,D0I,EMV,EMI,SFV,EFV
      READ(LIN,1) DN1,DN2,DN3,DL4
      READ(LIN,1) GP
C
C  FOR FACE-CENTERED CUBIC METALS
C
      O=(A0**3)/4.D0
      BV=A0/DSQRT(3.D0)
      BVS=BV*BV
      SBN=SM*BV/(4.D0*PI*(1.D0-PR))
      RC=BV*RC0
      RCP=RC*(1.D0+DL4I)
      M=27
      N=M*4
C
C  DEFECT GENERATION RATE AS A FRACTION, FC, OF ATOMIC DISPLACEMENT RATE
C  ESTIMATED FROM THE INITIAL DAMAGE ENERGY, GP, CALCULATED BY E-DEP-1
C
C  TRANSFORMATION OF DEPTH POSITION COORDINATE AND
C  INTERPOLATION OF DEFECT GENERATION RATE
C
      IM=131
      XI=IM
      GPS=0.D0
      CF=2.5D-3
      FC=0.2D0
      DO 200 I=1,IM
      GP(I)=GP(I)*CF*FC
  200 GPS=GPS+GP(I)
      GPA=GPS/XI
      DO 60 I=1,M
      IF(X(I).GT.1.3D0) GO TO 62
      XI=X(I)*100.D0
      IX=XI
      XD=XI-IX
      IF(XD.GT.0.5D0) IX=IX+1
      IM=IX+1
      G(I)=GP(IM)
      GO TO 60
   62 G(I)=0.D0
   60 DX(I)=X(I+1)-X(I)
C
C  DETERMINATION OF PARAMETERS FOR FINITE DIFFERENCE QUOTIENTS
C  WHEN DV AND DI ARE INDEPENDENT OF X
C
      CF=1.D-4
      DO 90 K=1,M
   90 DX(K)=DX(K)*CF
      DO 63 K=2,M
      ALP(K)=2.D0/(DX(K-1)*(DX(K)+DX(K-1)))
      GAM(K)=2.D0/(DX(K)*(DX(K)+DX(K-1)))
   63 BET(K)=ALP(K)+GAM(K)
C
C  TEMPERATURE DEPENDENT DEFECT PARAMETERS
C
```

```
      RZ=R0*A0
      AKT=BB*TM
      BKT=BC*TM
      DV=D0V*DEXP(-EMV/BKT)
      DI=D0I*DEXP(-EMI/BKT)
      R=4.D0*PI*RZ*(DI*DV)/O
      CVE=DEXP(SFV)*DEXP(-EFV/BKT)
C
C  SINK PARAMETERS
C
      RSL=((3.D0/(4.D0*PI*DN1))**EX3)/BV
      R4=1.D0/DSQRT(PI*DL4)
      ZV=2.D0*PI/DLOG(R4/RC)
      ZI=2.D0*PI/DLOG(R4/RCP)
C
C  PARAMETERS FOR GEAR-B
C
      T0=0.D0
      TL=1.68D+3
      H0=1.D-10
      EPS=1.D-9
      MF=22
      WRITE(LOUT,10) A0,RCO,RV0,TM,R0,SM,PR,SE,SF,D0V,EMV,DV,D0I,EMI,DI,
     ASFV,EFV,CVE,DN1,DN2,DN3,DL4,DL4I,T0,TL,EPS,H0,MF
   10 FORMAT(1H1/90H GROWTH KINETICS OF DEFECT CLUSTERS IN A SEMI-INFINI
     ATE MEDIUM DURING HEAVY ION IRRADIATION///
     B 5X,12H   A0(CM) = ,E10.4,5X,10H RC(BV) = ,F4.2,
     C 5X,11H RV0(BV) = ,F4.2//
     D 4X,12H    TM(K) = ,F7.1,9X,10H R0(A0) = ,F4.2//
     E 7X,17H SM(DYNES/CM2) = ,E10.4,5X,6H PR = ,F6.4//
     F 7X,16H SE(ERGS/CM2) = ,E10.4,5X,16H SF(ERGS/CM2) = ,E10.4//
     G 7X,14H D0V(CM2/S) = ,E10.4,5X,11H EMV(EV) = ,F4.2,5X,13H DV(CM2/S
     H) = ,E10.4//
     I 7X,14H D0I(CM2/S) = ,E10.4,5X,11H EMI(EV) = ,F4.2,5X,13H DI(CM2/S
     J) = ,E10.4//
     K 7X,11H SFV(BC) = ,F4.2,5X,11H EFV(EV) = ,F4.2,5X,6HCVE = ,E10.4//
     L 7X,13H DN1(CM-3) = ,E10.4,5X,13H DN2(CM-3) = ,E10.4,
     M 5X,13H DN3(CM-3) = ,E10.4//7X,13H DL4(CM-2) = ,E10.4,
     N 5X,8H DL4I = ,F4.2//
     O 7X,5H T0 =,E8.2,2X,5H TL =,E8.2,5X,5HEPS =,E8.2,5X,5H H0 =,E8.2,
     P 5X,5H MF =,I3//)
      WRITE(LOUT,70) (K,X(K),K=1,M)
   70 FORMAT(//55X,5H X(K),//5(I4,E16.5,6X))
      WRITE(LOUT,71) (K,G(K),K=1,M)
   71 FORMAT(//55X,5H G(K),//5(I4,E16.5,6X))
      WRITE(LOUT,72) (K,DX(K),K=1,M)
   72 FORMAT(//55X,6H DX(K),//5(I4,E16.5,6X))
C
C  INITIAL CONDITIONS:
C  R10 = RADIUS OF INTERSTITIAL TYPE LOOPS (BV)
C  R20 = RADIUS OF VACANCY TYPE LOOPS (BV)
C  R30 = RADIUS OF VOIDS (BV)
C  CV0 = VACANCY CONCENTRATION (ATOM FRACTION)
C  CI0 = INTERSTITIAL CONCENTRATION (ATOM FRACTION)
C  GN = NUMBER OF GAS ATOMS IN AN EQUILIBRIUM BUBBLE OF RADIUS R30
C
      R30=5.D0
      R10=DSQRT(4.D0/3.D0*DN3/DN1*R30**3)
```

```
      GN=8.D0*PI*SF*R30*R30*BVS/(3.D0*(AKT+2.D0*SF*BF/(R30*BV)))
      CI0=0.D0
      CV0=0.D0
      DO 100 K = 1,M
      KV=4*K-3
      KI=KV+1
      K1=KI+1
      K3=K1+1
      Y0(KV)=CV0+CVE
      Y0(KI)=CI0
      Y0(K1)=R10
      Y0(K3)=R30
      CV(K)=Y0(KV)
      CI(K)=Y0(KI)
      DCD(K)=DV*CV(K)-DI*CI(K)
      R1(K)=Y0(K1)
  100 R3(K)=Y0(K3)
      WRITE(LOUT,40) T0
   40 FORMAT(1H1//4H T =,E15.8)
      WRITE(LOUT,41) (K,CV(K),K=1,M)
   41 FORMAT(//55X,6H CV(K),//5(I4,E16.5,6X))
      WRITE(LOUT,42) (K,CI(K),K=1,M)
   42 FORMAT(//55X,6H CI(K),//5(I4,E16.5,6X))
      WRITE(LOUT,46) (K,DCD(K),K=1,M)
   46 FORMAT(//55X,7H DCD(K),//5(I4,E16.5,6X))
      WRITE(LOUT,43) (K,R1(K),K=1,M)
   43 FORMAT(//55X,6H R1(K),//5(I4,E16.5,6X))
      WRITE(LOUT,45) (K,R3(K),K=1,M)
   45 FORMAT(//55X,6H R3(K),//5(I4,E16.5,6X))
      C1(1)=CVE
      C3(1)=CVE
      INDEX=1
      ML=4
      MU=4
      ID=0
   50 ID=ID+1
      TOUT=TT(ID)
      CALL DRIVEB (N,T0,H0,Y0,TOUT,EPS,MF,INDEX,ML,MU)
C
C  OUTPUTS:
C  T = IRRADIATION TIME (SEC)
C  CV = VACANCY CONCENTRATION (ATOM FRACTION)
C  CI = INTERSTITIAL CONCENTRATION (ATOM FRACTION)
C  DCD = DV*(CV+CVE)-DI*CI (CM2/SEC)
C  R1 = INTERSTITIAL LOOP RADIUS (BV)
C  R3 = VOID RADIUS (BV)
C  C1 = LOCAL CONCENTRATION OF THERMAL VACANCIES AT INTERSITIAL LOOPS
C  C3 = LOCAL CONCENTRATION OF THERMAL VACANCIES AT VOIDS
C
      DO 101 K = 1,M
      KV=4*K-3
      KI=KV+1
      K1=KI+1
      K3=K1+1
      CV(K)=Y0(KV)
      CI(K)=Y0(KI)
      DCD(K)=DV*CV(K)-DI*CI(K)
      R1(K)=Y0(K1)
```

```
  101 R3(K)=YO(K3)
      WRITE(LOUT,40) TOUT
      WRITE(LOUT,41) (K,CV(K),K=1,M)
      WRITE(LOUT,42) (K,CI(K),K=1,M)
      WRITE(LOUT,46) (K,DCD(K),K=1,M)
      WRITE(LOUT,39) (K,C1(K),K=1,M)
   39 FORMAT(//55X,6H C1(K),//5(I4,E16.5,6X))
      WRITE(LOUT,38) (K,C3(K),K=1,M)
   38 FORMAT(//55X,6H C3(K),//5(I4,E16.5,6X))
      WRITE(LOUT,40) TOUT
      WRITE(LOUT,43) (K,R1(K),K=1,M)
      WRITE(LOUT,45) (K,R3(K),K=1,M)
C
C  AVERAGING OF LOOP AND VOID RADII AND SINK STRENGTH CONSTANTS
C  WITH RESPECT TO PETETRATION DEPTH
C
      R1A=0.D0
      R3A=0.D0
      DXA=0.D0
      S1A=0.D0
      S2A=0.D0
      DO 102 K=2,20
      DXA=DXA+DX(K-1)
      S1A=S1A+SS1(K)*DX(K-1)
      S2A=S2A+SS2(K)*DX(K-1)
      R1A=R1A+R1(K)*DX(K-1)
  102 R3A=R3A+R3(K)*DX(K-1)
      R1A=R1A/DXA
      R3A=R3A/DXA
      S1A=S1A/DXA
      S2A=S2A/DXA
C
C  EVALUATION OF IRRADIATION DOSE(DPA) AND VOID SWELLING(%)
C
      DOSE=GPA*TOUT
      DOSEF=G(6)*TOUT
      DOSEP=G(13)*TOUT
      DOSEB=G(17)*TOUT
      SZ=4.D0/3.D0*PI*DN3
      SW=SZ*(R3A*BV)**3
      SWF=SZ*(R3(6)*BV)**3
      SWP=SZ*(R3(13)*BV)**3
      SWB=SZ*(R3(17)*BV)**3
      SV=SW/(1.D0-SW)*100.D0
      SVF=SWF/(1.D0-SWF)*100.D0
      SVP=SWP/(1.D0-SWP)*100.D0
      SVB=SWB/(1.D0-SWB)*100.D0
      SW=SW*100.D0
      SWF=SWF*100.D0
      SWP=SWP*100.D0
      SWB=SWB*100.D0
C
C  OUTPUTS: COMPUTED RESULTS FOR AVERAGE AND 3 REFERENCE POSITIONS
C
      WRITE(LOUT,49)
   49 FORMAT(///24X,'AVERAGE',15X,'FRONT',18X,'PEAK',18X,'BACK'/)
      WRITE(LOUT,32) X(6),X(13),X(17)
   32 FORMAT(/4X,'X',27X,3(6X,E16.5))
```

```
      WRITE(LOUT,37) GPA,G(6),G(13),G(17)
   37 FORMAT(/4X,'G ',4X,4(6X,E16.5))
      WRITE(LOUT,33) DOSE,DOSEF,DOSEP,DOSEB
   33 FORMAT(/4X,'DOSE',2X,4(6X,E16.5))
      WRITE(LOUT,35) S1A,SS1(6),SS1(13),SS1(17)
   35 FORMAT(/4X,'S1',4X,4(6X,E16.5))
      WRITE(LOUT,34) S2A,SS2(6),SS2(13),SS2(17)
   34 FORMAT(/4X,'S2',4X,4(6X,E16.5))
      WRITE(LOUT,48) R1A,R1(6),R1(13),R1(17)
   48 FORMAT(/4X,'R1',4X,4(6X,E16.5))
      WRITE(LOUT,47) R3A,R3(6),R3(13),R3(17)
   47 FORMAT(/4X,'R3',4X,4(6X,E16.5))
      WRITE(LOUT,36) SW,SWF,SWP,SWB
   36 FORMAT(/4X,'SW',4X,4(6X,E16.5))
      WRITE(LOUT,51) SV,SVF,SVP,SVB
   51 FORMAT(/4X,'SV',4X,4(6X,E16.5))
      IF(TOUT.LT.TL) GO TO 50
      IF (INDEX .NE. 0) GO TO 80
   80 WRITE(LOUT,30) NSTEP,NFE,NJE
   30 FORMAT(//21H PROBLEM COMPLETED IN,I6,6H STEPS/
     1          21X,I6,14H F EVALUATIONS/
     2          21X,I6,14H J EVALUATIONS///)
      STOP
      END
```

```
      SUBROUTINE DIFFUN (N, T, Y, YDOT)
C
C  A SYSTEM OF N FIRST-ORDER ORDINARY DIFFERENTIAL RATE EQUATIONS
C  THIS SUBROUTINE CALLS NO OTHER SUBROUTINES
C
      IMPLICIT REAL*8 (A-H,O-Z)
      COMMON /GEARA/ R,O,BV,DV,DI,RCO,RVO,CVE,M
      COMMON /GEARB/ DN1,DN2,DN3,DL4,SBN,SE,SF,GN,BF
      COMMON /GEARC/ PI,AKT,BVS,RSL,ZV,ZI
      COMMON /GEARD/ SS1(27),SS2(27),ALP(27),BET(27),GAM(27),G(27)
      COMMON /GEARE/ C1(27),C3(27)
      DIMENSION Y(N),YDOT(N)
      DO 100 K=1,M
      KV=4*K-3
      KI=KV+1
      K1=KI+1
      K3=K1+1
      IF(K.NE.1) GO TO 11
      YDOT(KV)=0.D0
      YDOT(KI)=0.D0
      YDOT(K1)=0.D0
      YDOT(K3)=0.D0
      GO TO 100
C
C  THE SINK STRENGTH COEFFICIENTS
C
   11 SS11=0.D0
      SS13=0.D0
      SS14=ZV*DL4
      SS21=0.D0
      SS23=0.D0
      SS24=ZI*DL4
      IF(Y(K1).LE.RCO) GO TO 19
      SS11=2.D0*PI*DN1*Y(K1)*BV*ZV
      SS21=2.D0*PI*DN1*Y(K1)*BV*ZI
   19 IF(Y(K3).LE.RVO) GO TO 20
      SS13=4.D0*PI*Y(K3)*BV*DN3
      SS23=SS13
   20 SS1(K)=SS11+SS13+SS14
      SS2(K)=SS21+SS23+SS24
C
C  LOCAL CONCENTRATIONS OF THERMAL VACANCIES AT LOOPS AND VOIDS
C  INTERSTITIAL LOOPS UNFAULT WHEN THEIR RADII EXCEED RSL
C
      IF(Y(K1).LE.RCO) GO TO 31
      IF(Y(K1).GT.RSL) GO TO 37
      C1(K)=CVE*DEXP(-O/(BV*AKT)*(SE+SBN*DLOG(Y(K1))/Y(K1)))
      GO TO 34
   37 C1(K)=CVE*DEXP(-O*SBN/(BV*AKT)*DLOG(Y(K1))/Y(K1))
      GO TO 34
   31 C1(K)=0.D0
   34 IF(Y(K3).LE.RVO ) GO TO 35
      PG=GN*AKT/(4.D0/3.D0*PI*(Y(K3)*BV)**3-GN*BF)
      IF(PG.LT.0.D0) PG=0.D0
      C3(K)=CVE*DEXP(O/AKT*(2.D0*SF/(Y(K3)*BV)-PG))
      GO TO 36
```

```
   35 C3(K)=0.D0
C
C  RATE EQUATIONS IN A VECTOR FORM FOR VACANCIES AND INTERSTITIALS
C
   36 IF(K.LT.M) GO TO 12
      YDOT(KV)=DV*(ALP(K)*Y(KV-4)-BET(K)*Y(KV)+GAM(K)*CVE)
     A+G(K)-R*Y(KV)*Y(KI)-DV*(SS11*(Y(KV)-C1(K))+SS13*(Y(KV)-C3(K))
     B+SS14*(Y(KV)-CVE))
      YDOT(KI)=DI*(ALP(K)*Y(KI-4)-BET(K)*Y(KI))
     A+G(K)-R*Y(KV)*Y(KI)-DI*SS2(K)*Y(KI)
      GO TO 13
   12 YDOT(KV)=DV*(ALP(K)*Y(KV-4)-BET(K)*Y(KV)+GAM(K)*Y(KV+4))
     A+G(K)-R*Y(KV)*Y(KI)-DV*(SS11*(Y(KV)-C1(K))+SS13*(Y(KV)-C3(K))
     B+SS14*(Y(KV)-CVE))
      YDOT(KI)=DI*(ALP(K)*Y(KI-4)-BET(K)*Y(KI)+GAM(K)*Y(KI+4))
     A+G(K)-R*Y(KV)*Y(KI)-DI*SS2(K)*Y(KI)
C
C  RATE EQUATIONS IN A VECTOR FORM FOR SINKS
C
   13 IF(Y(K1).LE.RCO) GO TO 41
      YDOT(K1)=(DI*Y(KI)*ZI-DV*(Y(KV)-C1(K))*ZV)/BVS
      GO TO 44
   41 YDOT(K1)=0.D0
   44 IF(Y(K3).LE.RVO) GO TO 45
      YDOT(K3)=(DV*(Y(KV)-C3(K))-DI*Y(KI))/(Y(K3)*BVS)
      GO TO 100
   45 YDOT(K3)=0.D0
  100 CONTINUE
      RETURN
      END
```

```
      SUBROUTINE PDB (N, T, Y, PD, NO, ML, MU)
C
C  WHEN MF = 22, JACOBIAN MATRIX IS EVALUATED NUMERICALLY
C  THIS IS A DUMMY SUBROUTINE
C
      IMPLICIT REAL*8 (A-H,O-Z)
      DIMENSION PD(NO,NO)
      RETURN
      END
```

APPENDIX C

The print-outs for the last time-out are given in the following pages. Some of the important dimensions are as follows:

T	sec	irradiation time
X	μm	depth position
G	dpa/sec	defect generation rate
DX	μm	finite increment
CV	fraction	vacancy concentration
CI	fraction	interstitial concentration
DCD	cm^2/sec	$D_v(C_v + C_v^e) - D_i C_i$
R1	b	loop radius
R3	b	void radius
C1	fraction	thermal vacancy concentration at loops
C3	fraction	thermal vacancy concentration at voids
DOSE	dpa	irradiation dose
S1	cm^{-2}	sink strength for vacancies
S2	cm^{-2}	sink strength for interstitials
SW	%	void swelling $\Delta V/V \times 100$
SV	%	void swelling $\Delta V/(V - \Delta V) \times 100$

GROWTH KINETICS OF DEFECT CLUSTERS IN A SEMI-INFINITE MEDIUM DURING HEAVY ION IRRADIATION

AO(CM) = 0.3524D-07 RC(BV) = 2.00 RVO(BV) = 1.00

TM(K) = 823.0 RO(AO) = 1.20

SM(DYNES/CM2) = 0.9470D 12 PR = 0.2760

SE(ERGS/CM2) = 0.4000D 03 SF(ERGS/CM2) = 0.1000D 04

DOV(CM2/S) = 0.1900D 00 EMV(EV) = 1.20 DV(CM2/S) = 0.8571D-08

DOI(CM2/S) = 0.8000D-02 EMI(EV) = 0.15 DI(CM2/S) = 0.9658D-03

SFV(BC) = 1.50 EFV(EV) = 1.60 CVE = 0.7197D-09

DN1(CM-3) = 0.4000D 15 DN2(CM-3) = 0.1000D 13 DN3(CM-3) = 0.2000D 15

DL4(CM-2) = 0.1000D 11 DL4I = 0.60

TO =0.0 TL =0.17D 04 EPS =0.10D-08 HO =0.10D-09 NF = 22

X(K)

1	0.0	2	0.10000D-01	3	0.20000D-01	4	0.40000D-01	5	0.80000D-01
6	0.14000D 00	7	0.22000D 00	8	0.32000D 00	9	0.42000D 00	10	0.52000D 00
11	0.60000D 00	12	0.66000D 00	13	0.70000D 00	14	0.74000D 00	15	0.80000D 00
16	0.86000D 00	17	0.92000D 00	18	0.98000D 00	19	0.10400D 01	20	0.11000D 01
21	0.11600D 01	22	0.12400D 01	23	0.14000D 01	24	0.17000D 01	25	0.22000D 01
26	0.31000D 01	27	0.48000D 01						

G(K)

1	0.17470D-03	2	0.17685D-03	3	0.17905D-03	4	0.18360D-03	5	0.19335D-03
6	0.20985D-03	7	0.23630D-03	8	0.27975D-03	9	0.34235D-03	10	0.43705D-03
11	0.53235D-03	12	0.58890D-03	13	0.60045D-03	14	0.57995D-03	15	0.48465D-03
16	0.33990D-03	17	0.19490D-03	18	0.88700D-04	19	0.32150D-04	20	0.92500D-05
21	0.21000D-05	22	0.20000D-06	23	0.0	24	0.0	25	0.0
26	0.0	27	0.0						

DX(K)

1	0.10000D-05	2	0.10000D-05	3	0.20000D-05	4	0.40000D-05	5	0.60000D-05
6	0.80000D-05	7	0.10000D-04	8	0.10000D-04	9	0.10000D-04	10	0.80000D-05
11	0.60000D-05	12	0.40000D-05	13	0.40000D-05	14	0.60000D-05	15	0.60000D-05
16	0.60000D-05	17	0.60000D-05	18	0.60000D-05	19	0.60000D-05	20	0.60000D-05
21	0.80000D-05	22	0.16000D-04	23	0.30000D-04	24	0.50000D-04	25	0.90000D-04
26	0.17000D-03	27	0.32000D-03						

T = 0.0

CV(K)

1	0.71969D-09	2	0.71969D-09	3	0.71969D-09	4	0.71969D-09	5	0.71969D-09
6	0.71969D-09	7	0.71969D-09	8	0.71969D-09	9	0.71969D-09	10	0.71969D-09
11	0.71969D-09	12	0.71969D-09	13	0.71969D-09	14	0.71969D-09	15	0.71969D-09
16	0.71969D-09	17	0.71969D-09	18	0.71969D-09	19	0.71969D-09	20	0.71969D-09
21	0.71969D-09	22	0.71969D-09	23	0.71969D-09	24	0.71969D-09	25	0.71969D-09
26	0.71969D-09	27	0.71969D-09						

CI(K)

1	0.0	2	0.0	3	0.0	4	0.0	5	0.0
6	0.0	7	0.0	8	0.0	9	0.0	10	0.0
11	0.0	12	0.0	13	0.0	14	0.0	15	0.0
16	0.0	17	0.0	18	0.0	19	0.0	20	0.0
21	0.0	22	0.0	23	0.0	24	0.0	25	0.0
26	0.0	27	0.0						

DCD(K)

1	0.61684D-17	2	0.61684D-17	3	0.61684D-17	4	0.61684D-17	5	0.61684D-17
6	0.61684D-17	7	0.61684D-17	8	0.61684D-17	9	0.61684D-17	10	0.61684D-17
11	0.61684D-17	12	0.61684D-17	13	0.61684D-17	14	0.61684D-17	15	0.61684D-17
16	0.61684D-17	17	0.61684D-17	18	0.61684D-17	19	0.61684D-17	20	0.61684D-17
21	0.61684D-17	22	0.61684D-17	23	0.61684D-17	24	0.61684D-17	25	0.61684D-17
26	0.61684D-17	27	0.61684D-17						

R1(K)

1	0.91287D 01	2	0.91287D 01	3	0.91287D 01	4	0.91287D 01	5	0.91287D 01
6	0.91287D 01	7	0.91287D 01	8	0.91287D 01	9	0.91287D 01	10	0.91287D 01
11	0.91287D 01	12	0.91287D 01	13	0.91287D 01	14	0.91287D 01	15	0.91287D 01
16	0.91287D 01	17	0.91287D 01	18	0.91287D 01	19	0.91287D 01	20	0.91287D 01
21	0.91287D 01	22	0.91287D 01	23	0.91287D 01	24	0.91287D 01	25	0.91287D 01
26	0.91287D 01	27	0.91287D 01						

R3(K)

1	0.50000D 01	2	0.50000D 01	3	0.50000D 01	4	0.50000D 01	5	0.50000D 01
6	0.50000D 01	7	0.50000D 01	8	0.50000D 01	9	0.50000D 01	10	0.50000D 01
11	0.50000D 01	12	0.50000D 01	13	0.50000D 01	14	0.50000D 01	15	0.50000D 01
16	0.50000D 01	17	0.50000D 01	18	0.50000D 01	19	0.50000D 01	20	0.50000D 01
21	0.50000D 01	22	0.50000D 01	23	0.50000D 01	24	0.50000D 01	25	0.50000D 01
26	0.50000D 01	27	0.50000D 01						

T = 0.16800000D 04

CV(K)

1	0.71969D-09	2	0.85747D-07	3	0.15282D-06	4	0.24486D-06	5	0.34267D-06
6	0.42671D-06	7	0.49996D-06	8	0.57127D-06	9	0.64444D-06	10	0.72791D-06
11	0.79146D-06	12	0.81839D-06	13	0.81714D-06	14	0.79602D-06	15	0.72339D-06
16	0.60891D-06	17	0.47375D-06	18	0.34077D-06	19	0.20619D-06	20	0.11254D-06
21	0.57268D-07	22	0.21695D-07	23	0.40386D-08	24	0.91353D-09	25	0.72383D-09
26	0.71972D-09	27	0.71969D-09						

CI(K)

1	0.18794D-23	2	0.71761D-12	3	0.12768D-11	4	0.20276D-11	5	0.28012D-11
6	0.34664D-11	7	0.40527D-11	8	0.46276D-11	9	0.52194D-11	10	0.58963D-11
11	0.64131D-11	12	0.66320D-11	13	0.66230D-11	14	0.64528D-11	15	0.58646D-11
16	0.49357D-11	17	0.38357D-11	18	0.27515D-11	19	0.16403D-11	20	0.87423D-12
21	0.42993D-12	22	0.15204D-12	23	0.22164D-13	24	0.11760D-14	25	0.22677D-16
26	0.13364D-18	27	0.22268D-21						

DCD(K)

1	0.61684D-17	2	0.41884D-16	3	0.76707D-16	4	0.14046D-15	5	0.23175D-15
6	0.30956D-15	7	0.37111D-15	8	0.42714D-15	9	0.48272D-15	10	0.54446D-15
11	0.59004D-15	12	0.60938D-15	13	0.60736D-15	14	0.59071D-15	15	0.53625D-15
16	0.45221D-15	17	0.35611D-15	18	0.26341D-15	19	0.18310D-15	20	0.12030D-15
21	0.75630D-16	22	0.39111D-16	23	0.13209D-16	24	0.66942D-17	25	0.61821D-17
26	0.61685D-17	27	0.61684D-17						

C1(K)

1	0.71969D-09	2	0.81769D-10	3	0.89614D-10	4	0.63470D-09	5	0.62748D-09
6	0.88182D-10	7	0.84823D-10	8	0.83985D-10	9	0.85380D-10	10	0.88204D-10
11	0.90711D-10	12	0.62879D-09	13	0.63216D-09	14	0.63230D-09	15	0.62434D-09
16	0.88067D-10	17	0.78424D-10	18	0.0	19	0.0	20	0.0
21	0.0	22	0.0	23	0.0	24	0.0	25	0.0
26	0.0	27	0.0						

C3(K)

1	0.71969D-09	2	0.12780D-08	3	0.10661D-08	4	0.95360D-09	5	0.89125D-09
6	0.86339D-09	7	0.84902D-09	8	0.83926D-09	9	0.83156D-09	10	0.82462D-09
11	0.82034D-09	12	0.81881D-09	13	0.81906D-09	14	0.82058D-09	15	0.82597D-09
16	0.83607D-09	17	0.85234D-09	18	0.87691D-09	19	0.91387D-09	20	0.96995D-09
21	0.10583D-08	22	0.12924D-08	23	0.15498D-08	24	0.78133D-09	25	0.72128D-09
26	0.71970D-09	27	0.71969D-09						

T = 0.16800000D 04

R1(K)

1	0.91287D 01	2	0.21375D 03	3	0.36774D 03	4	0.50172D 03	5	0.45231D 03
6	0.32832D 03	7	0.25851D 03	8	0.24471D 03	9	0.26818D 03	10	0.32857D 03
11	0.40362D 03	12	0.46039D 03	13	0.48325D 03	14	0.48421D 03	15	0.43308D 03
16	0.32528D 03	17	0.17700D 03	18	0.20000D 01	19	0.20000D 01	20	0.20000D 01
21	0.20000D 01	22	0.20000D 01	23	0.20000D 01	24	0.20000D 01	25	0.20000D 01
26	0.20000D 01	27	0.20000D 01						

R3(K)

1	0.50000D 01	2	0.16284D 02	3	0.24123D 02	4	0.33862D 02	5	0.44678D 02
6	0.52521D 02	7	0.57880D 02	8	0.62251D 02	9	0.66234D 02	10	0.70325D 02
11	0.73125D 02	12	0.74182D 02	13	0.74011D 02	14	0.72957D 02	15	0.69485D 02
16	0.63833D 02	17	0.56539D 02	18	0.48371D 02	19	0.39960D 02	20	0.31914D 02
21	0.24593D 02	22	0.15957D 02	23	0.53371D 01	24	0.50205D 01	25	0.50005D 01
26	0.50000D 01	27	0.50000D 01						

	AVERAGE	FRONT	PEAK	BACK
X		0.14000D 00	0.70000D 00	0.92000D 00
G	0.26498D-03	0.20985D-03	0.60045D-03	0.19490D-03
DOSE	0.44516D 00	0.35255D 00	0.10088D 01	0.32743D 00
S1	0.34399D 11	0.36886D 11	0.48122D 11	0.27220D 11
S2	0.37702D 11	0.40488D 11	0.52792D 11	0.29782D 11
R1	0.28506D 03	0.32832D 03	0.48325D 03	0.17700D 03
R3	0.59379D 02	0.52521D 02	0.74011D 02	0.56539D 02
SE	0.14773D 00	0.10223D 00	0.28607D 00	0.12753D 00
SV	0.14795D 00	0.10233D 00	0.28689D 00	0.12770D 00

PROBLEM COMPLETED IN 4515 STEPS
21536 F EVALUATIONS
1513 J EVALUATIONS

IHC002I STOP 0

ORNL/TM-5789
Distribution
Category UC-25

INTERNAL DISTRIBUTION

1–2. Central Research Library
3. Document Reference Section
4–12. Laboratory Records Department
13. Laboratory Records, ORNL RC
14. ORNL Patent Office
15. W. H. Butler
16. R. W. Carpenter
17. W. A. Coghlan
18. J. E. Cunningham
19. K. Farrell
20. J. S. Faulkner
21. R. W. Hendricks
22–24. M. R. Hill
25. E. A. Kenik
26. C. C. Koch
27. L. K. Mansur
28. C. J. McHargue
29. J. Narayan
30. T. S. Noggle
31. O. S. Oen
32. S. M. Ohr
33. N. H. Packan
34. M. T. Robinson
35. A. F. Rowcliffe
36. J. O. Stiegler
37. D. B. Trauger
38. J. R. Weir, Jr.
39. F. W. Wiffen
40. M. K. Wilkinson
41–55. M. H. Yoo
56. F. W. Young, Jr.
57. A. Zucker
58. R. W. Balluffi (consultant)
59. P. M. Brister (consultant)
60. W. R. Hibbard (consultant)
61. John Moteff (consultant)
62. Hayne Palmour III (consultant)
63. N. E. Promisel (consultant)
64. D. F. Stein (consultant)

EXTERNAL DISTRIBUTION

65. R. J. Arsenault, Engineering Materials Group, University of Maryland, College Park, MD 20742
66. J. R. Beeler, Jr., Department of Nuclear Engineering, North Carolina State University, Raleigh, NC 27607
67. A. L. Bement, Department of Metallurgical and Materials Science, Massachusetts Institute of Technology, Cambridge, MA 02139
68. A. D. Brailsford, Ford Scientific Laboratory, P.O. Box 2053, Dearborn, MI 48120
69. J. L. Brimhall, Batelle Pacific Northwest Laboratories, Richland, WA 99352
70. R. Bullough, Theoretical Physics Division, Bldg. B.9, Atomic Energy Research Establishment, Harwell, Birkshire, England
71. L. T. Chadderton, Physics Lab II, H. G. Orsted Institute, University of Copenhagen, Universitetsparken 5, DK-2100, Copenhagen ϕ, Denmark
72. J. W. Corbett, Physics Department, State University of New York at Albany, Albany, NY 12203
73. D. deFontaine, Materials Department, UCLA School of Engineering, Los Angeles, CA 90024
74. J. Dienes, Department of Physics, Brookhaven National Laboratory, Upton, NY 11973

75. R. Dutton, Materials Science Branch, Whiteshell Nuclear Research Establishment, Atomic Energy of Canada Limited, Pinawa, Manitoba, Canada
76. F. A. Garner, Hanford Engineering Development Laboratory, Richland, WA 99352
77. A. Goland, Brookhaven National Laboratory, Upton, NY 11973
78. R. A. Johnson, Department of Materials Science, University of Virginia, Charlottsville, VA 22903
79. W. G. Johnston, General Electric, Research and Development Center, P.O. Box 1, Schenectady, NY 12301
80. Adam Jostons, Australian Atomic Energy, Commission Research Establishment, Lucas Heights, New South Wales, Australia
81. G. Kulcinski, Nuclear Engineering Department, University of Wisconsin, Madison, WI 53706
82. M. Meshii, The Technical Institute, Department of Materials Science, Northwestern University, Evanston, IL 60201
83. T. E. Mitchell, Division of Metallurgy and Materials Science, Case Western Reserve University, University Circle, Cleveland, OH 44106
84. F. A. Nichols, Materials Science Division, Argonne National Laboratory, Argonne, IL 60439
85. W. Schilling, Institut für Festkörperforschung der Kernforschungsanlage, Jülich GmbH, D-5170 Jülich 1, Postfach 1913, Federal Republic of Germany
86. A. Seeger, Max-Planck-Institue für Metallforschung, Institue für Physik, D7000 Stuttgart 80, Büsnauer Strasse 171, W. Germany BRD
87. K. Shiraishi, Japan Atomic Energy Research Institute, Tokai-mura, Ibaraki-ken, Japan
88. B. N. Singh, Metallurgy Division, Danish Atomic Energy Commission, Research Establishment RISO, Roskilde, Denmark
89. R. E. Smallman, Department of Physical Metallurgy and Science of Materials, University of Birmingham, P.O. Box 363, Birmingham B15 2TT England
90. A. Sosin, Universtiy of Utah, Salt Lake City, UT 84117
91. J. A. Sprague, Naval Research Laboratory, Code 6395, Washington, DC 20375
92. J. T. Stanley, College of Engineering Science, Arizona State University, Tempe, AZ 85281
93. J. Washburn, Department of Materials Science and Engineering, College of Engineering, University of California, Berkeley, CA 94720
94. M. S. Wechsler, Department of Materials Science and Engineering, Iowa State University, Ames, IA 50010
95. H. Wiedersich, Materials Science Division, Argonne National Laboratory, Argonne, IL 60439
96. W. G. Wolfer, Department of Nuclear Engineering, Engineering Research Building, University of Wisconsin, Madison, WI 53706

97–99. ERDA, Division of Physical Research, Washington, DC 20545
L. C. Ianniello
D. K. Stevens
M. C. Wittels

100–101. ERDA, Oak Ridge Operations Office, P.O. Box E, Oak Ridge, TN 37830
Director
Research and Technical Support Division

102–345. ERDA, Technical Information Center, Office of Information Services, P.O. Box 62, Oak Ridge, TN 37830
For distribution as shown in TID-4500 Distribution Category, UC-25 (Materials)